Part IV:Application to the Lunar Core.

Lecture by J. Noir at WITGAF Cargese, Corsica, 2019

1. Geophysical motivations.
2. The uniform vorticity flow.
3. Parametric versus Boundary layer instability.
4. The dynamics of lunar core over the last 4Ga.

Part IV:Application to the Lunar Core.

Lecture by J. Noir at WITGAF Cargese, Corsica, 2019

1. Geophysical motivations.
2. The uniform vorticity flow.
3. Parametric versus Boundary layer instability.
4. The dynamics of lunar core over the last 4Ga.

Large dissipation in the lunar interior.

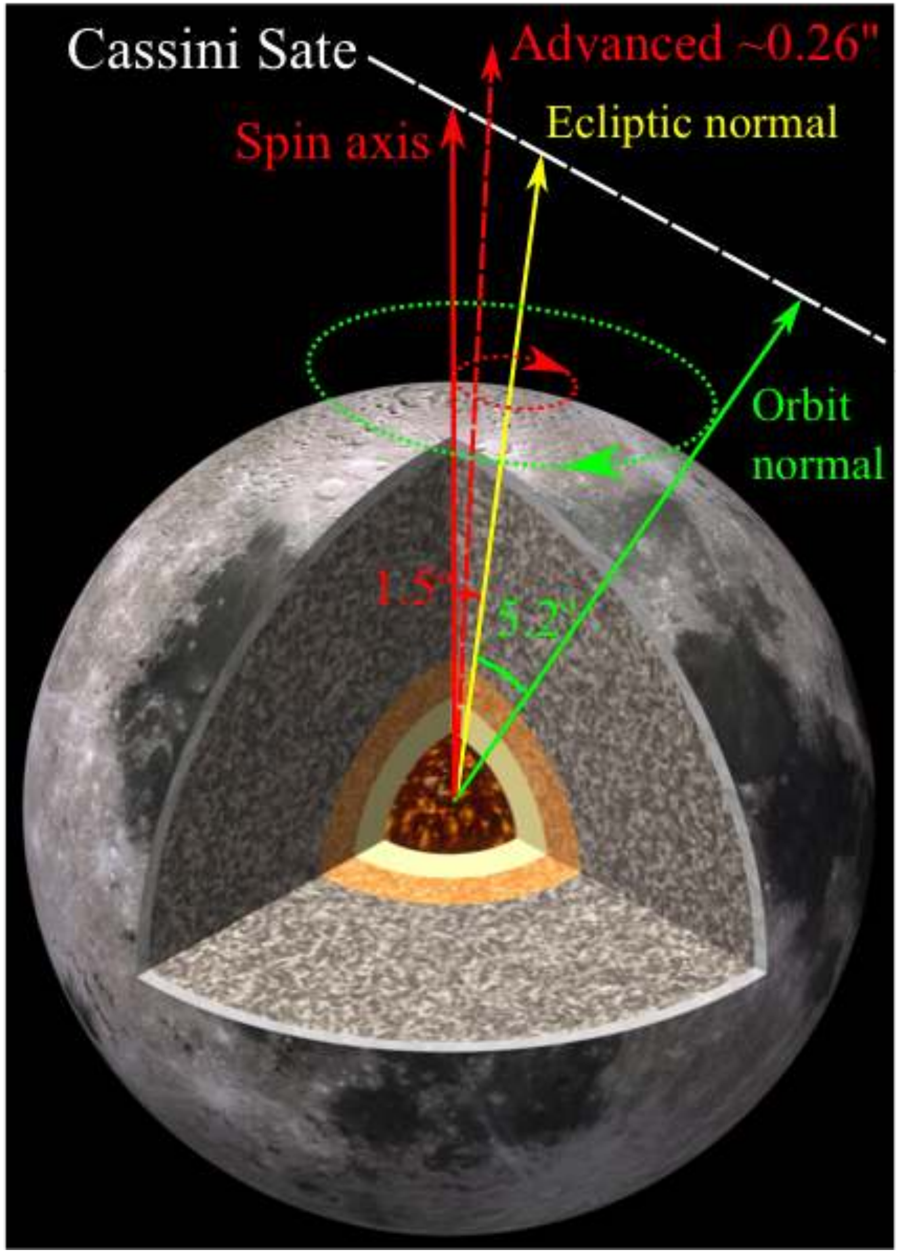

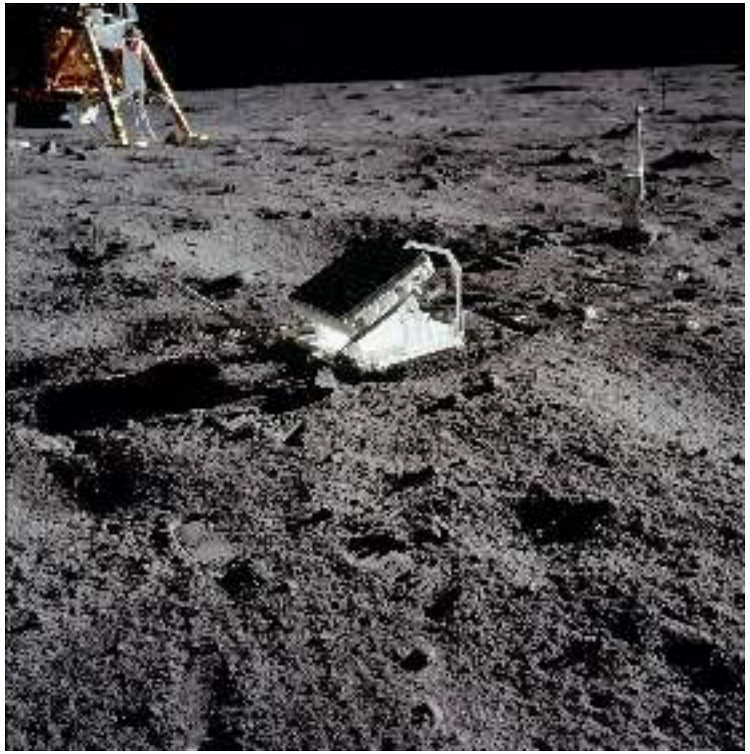

Credit: NASA

P ~ 76MW

This amount of dissipation is too large to be explained by a visco-elastic behaviour in a silicate mantle. It thus suggest it could results from dissipation in a liquid core.

Part IV:Application to the Lunar Core.

Lecture by J. Noir at WITGAF Cargese, Corsica, 2019

1. Geophysical motivations.
2. The uniform vorticity flow.
3. Parametric versus Boundary layer instability.
4. The dynamics of lunar core over the last 4Ga.

As the mantle precesses, the core remains in rotation but along a slightly tilted axis.

Sloudsky 1895, Poincare 1910, Busse 1968,
Noir and Cebron 2015, Cebron et al 2019.

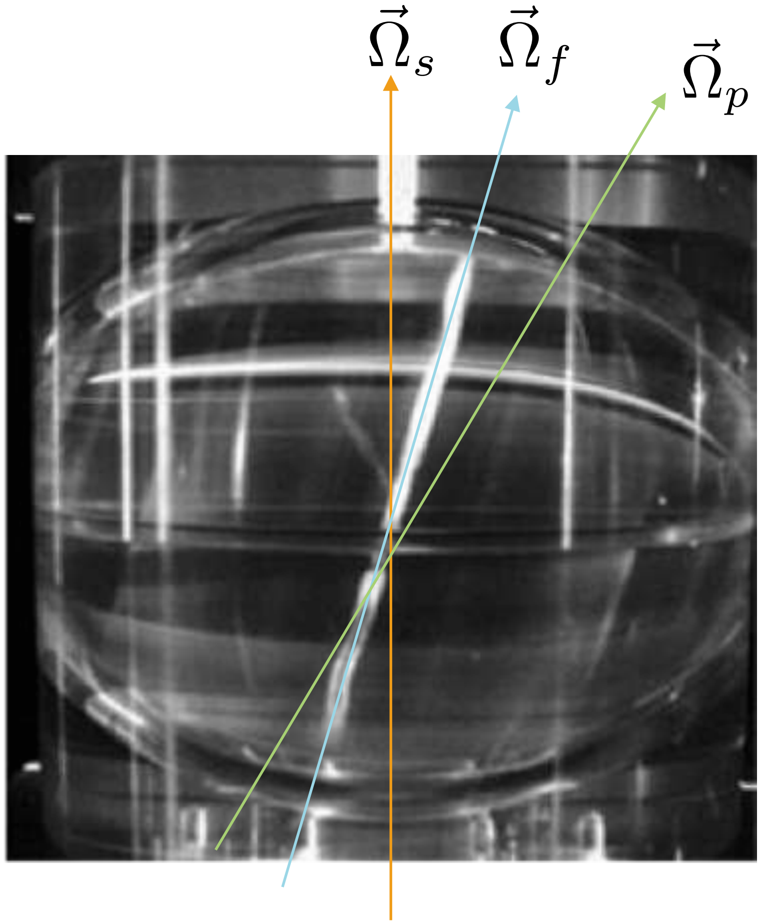

$$\vec{u} = \vec{\Omega}_f \times \vec{r} + \vec{\nabla}\phi$$

In the frame of precession, i.e. the turntable, the rotation of the fluid and of the mantle are fixed, viewed from the lab both axis are precessing at the same rate.

Let's look at the equations in the frame attached to the mantle, i.e. rotating at : $\vec{\Omega} = \vec{\Omega}_s + \vec{\Omega}_p$

Control parameters

$$\eta = \frac{a-c}{a} \sim 10^{-4}$$

$$E = \frac{\nu}{\Omega_s a^2} \sim 10^{-12}$$

$$Po = \frac{\Omega_p}{\Omega_s} \sim -10^{-4}$$

$$\alpha = 1.5^\circ$$

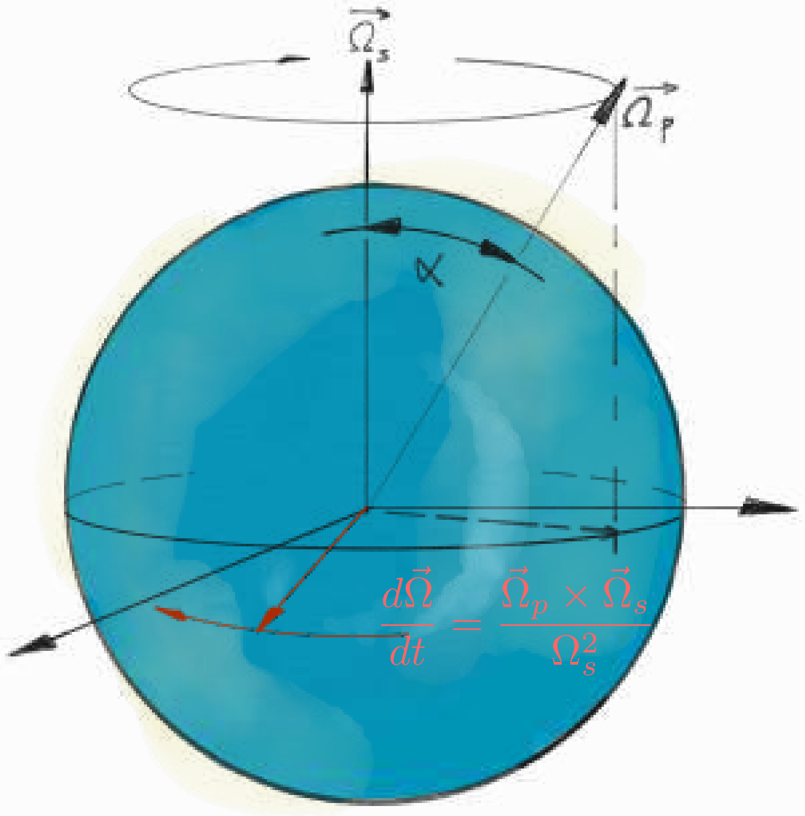

$$\frac{\partial \vec{u}}{\partial t} + 2\vec{\Omega} \times \vec{u} = -\vec{\nabla}\Pi + E\vec{\nabla}^2\vec{u} + \vec{r} \times \frac{d\vec{\Omega}}{dt}$$

$$\vec{\nabla} \cdot \vec{u} = 0$$

$\vec{u} = 0$ At the surface

$$\frac{d\vec{\Omega}}{dt} = \frac{\vec{\Omega}_p \times \vec{\Omega}_s}{\Omega_s^2}$$

Viewed from an observer fixed on the mantle, this vector travels in a retrograde direction with the period of rotation of the mantle:

The Poincare acceleration takes the form of a solid body rotation and appears as a forcing term in the equations.

Let's look at the equations in the frame attached to the mantle, i.e. rotating at : $\vec{\Omega} = \vec{\Omega}_s + \vec{\Omega}_p$

Control parameters

$$\eta = \frac{a-c}{a} \sim 10^{-4}$$

$$E = \frac{\nu}{\Omega_s a^2} \sim 10^{-12}$$

$$Po = \frac{\Omega_p}{\Omega_s} \sim -10^{-4}$$

$$\alpha = 1.5^\circ$$

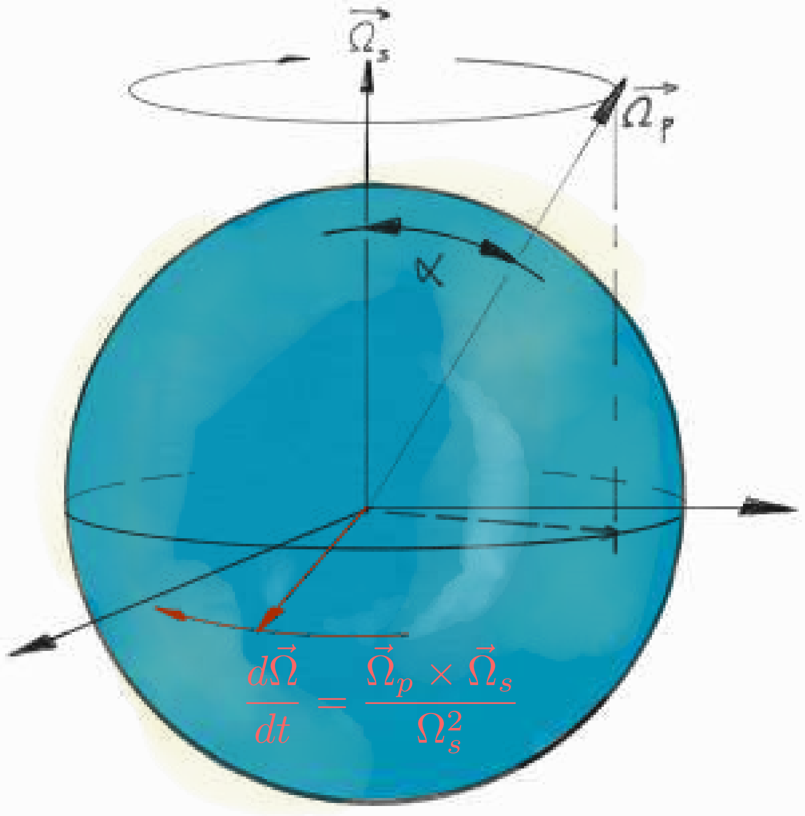

$$\frac{\partial \vec{u}}{\partial t} + 2\vec{\Omega} \times \vec{u} = -\vec{\nabla}\Pi + \vec{r} \times \frac{d\vec{\Omega}}{dt}$$

$$\frac{d\vec{\Omega}}{dt} = Posin\alpha(\cos(t)\hat{\mathbf{e}}_x + \sin(t)\hat{\mathbf{e}}_y)$$

$$\vec{\nabla} \cdot \vec{u} = 0$$

Poincaré mode:

$\vec{u}_{110} = \vec{\Omega}_{110} \times \vec{r}$ $\quad$ $\vec{u}_{110} = \vec{\Omega}_{110} \times \vec{r} + \vec{\nabla}\phi$

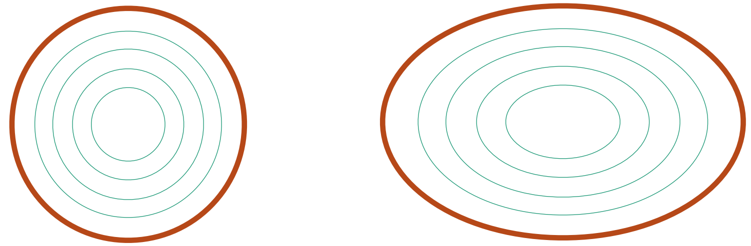

The Poincare acceleration takes the form of a solid body rotation and appears as a forcing term in the equations.

Let’s look at the equations in the frame attached to the mantle, i.e. rotating at : $\vec{\Omega} = \vec{\Omega}_s + \vec{\Omega}_p$

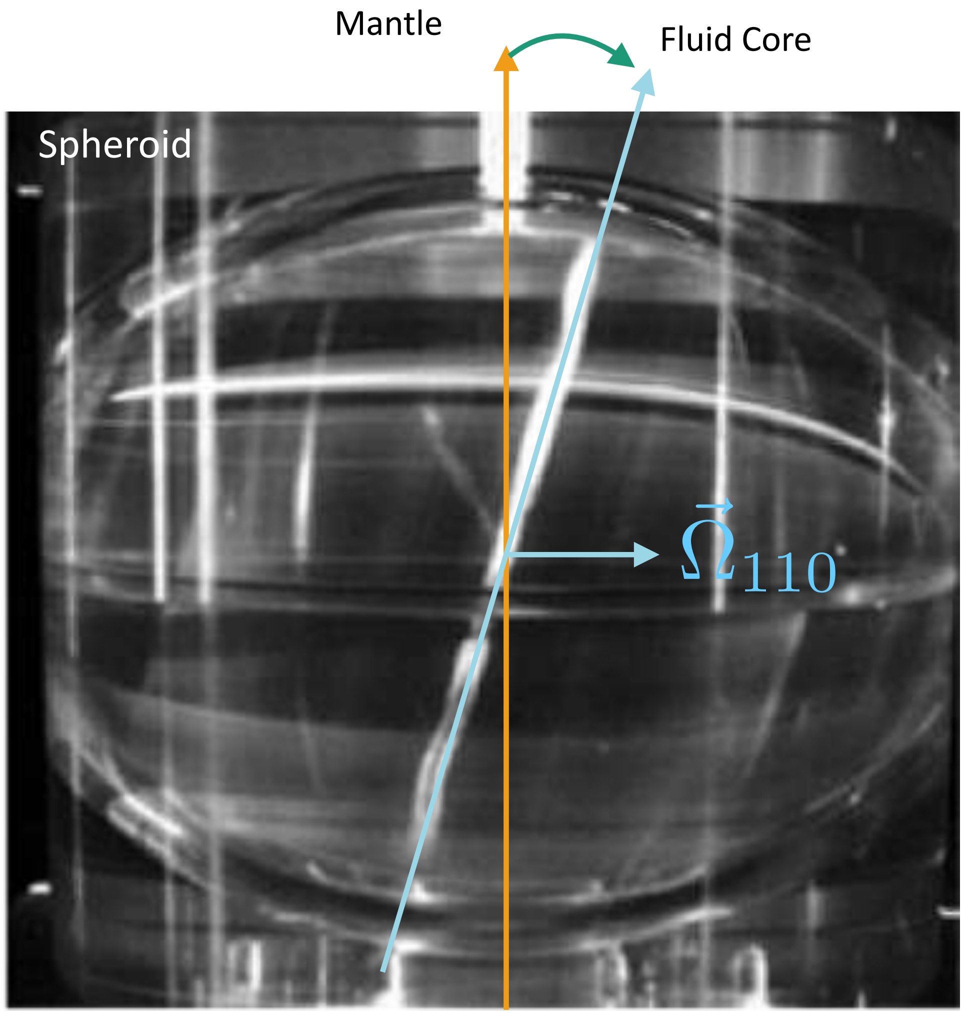

$$\frac{\partial \vec{u}}{\partial t} + 2\vec{\Omega} \times \vec{u} = -\vec{\nabla}\Pi + \vec{r} \times \frac{d\vec{\Omega}}{dt}$$

$$\frac{d\vec{\Omega}}{dt} = Posin\alpha(\cos(t)\hat{\mathbf{e}}_x + \sin(t)\hat{\mathbf{e}}_y)$$

$$\vec{\nabla} \cdot \vec{u} = 0$$

Poincaré mode:

$\vec{u}_{110} = \vec{\Omega}_{110} \times \vec{r}$

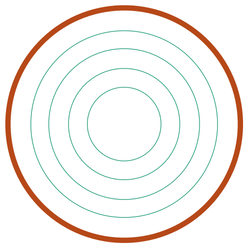

$\vec{u}_{110} = \vec{\Omega}_{110} \times \vec{r} + \vec{\nabla}\phi$

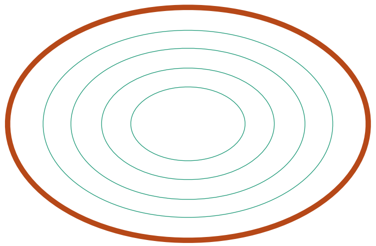

The Poincare acceleration takes the form of a solid body rotation and appears as a forcing term in the equations.

The flow of uniform vorticity: The Poincaré mode

$$\frac{\partial \vec{u}}{\partial t} + 2\vec{\Omega} \times \vec{u} = -\vec{\nabla}\Pi + E\vec{\nabla}^2\vec{u} + \boxed{\vec{r} \times \frac{d\vec{\Omega}}{dt}} \rightarrow \vec{u} = \vec{\Omega}_f \times \vec{r} + \vec{\nabla}\phi\,(\eta, \vec{\Omega}_f)$$

$$\vec{\nabla} \cdot \vec{u} = 0$$

Torque Balance approach (Busse 1968, Noir et al 2003, Noir and Cebron 2015)

$$\int_V \vec{r} \times \left[\frac{\partial \vec{u}}{\partial t} + 2\vec{\Omega} \times \vec{u} = -\vec{\nabla}\Pi + E\vec{\nabla}^2\vec{u} + \vec{r} \times \frac{d\vec{\Omega}}{dt} \right] dV$$

$$I_c \frac{d\vec{\Omega}_t}{dt} = \vec{\Gamma}_i + \vec{\Gamma}_p + \vec{\Gamma}_\nu + \vec{\Gamma}_{prec}$$

Viscous drag

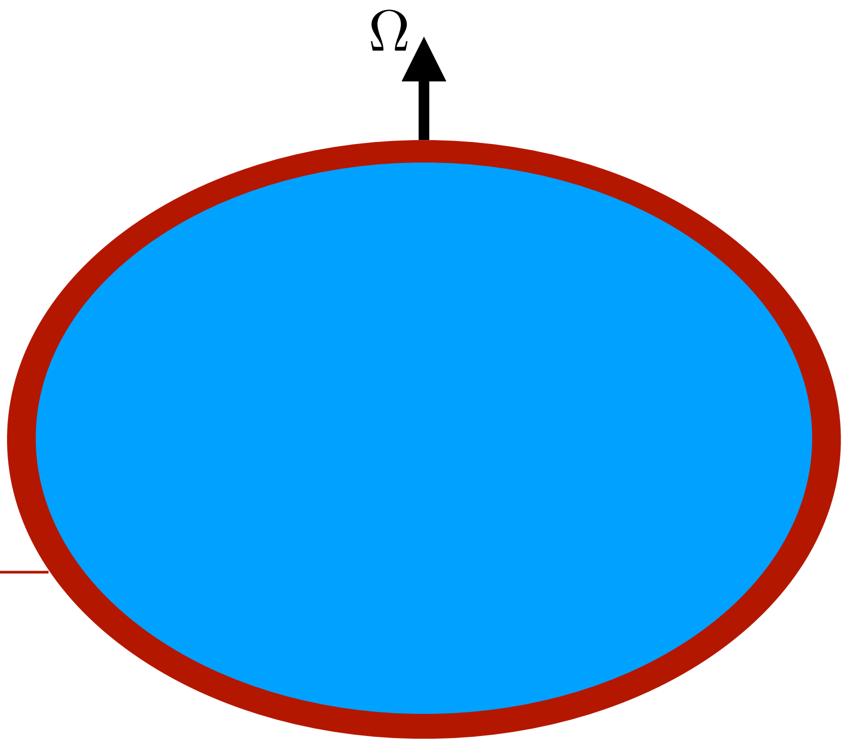

If the flow remains stable, i.e. of uniform vorticity:

$$\vec{\Gamma}_\nu = K(\vec{\Omega}_s - \vec{\Omega}_f) \qquad K = I_c \lambda_l \sqrt{E}$$

λ_l : decay rate of the Poincaré mode (Greenspan 1968, Zhang 2018, Vantieghem 2014, Rieutord 2011).

The flow of uniform vorticity: The Poincaré mode

$$\frac{\partial \vec{u}}{\partial t} + 2\vec{\Omega} \times \vec{u} = -\vec{\nabla}\Pi + E\vec{\nabla}^2\vec{u} + \vec{r} \times \frac{d\vec{\Omega}}{dt}$$

$$\vec{u} = \vec{\Omega}_f \times \vec{r} + \vec{\nabla}\phi\,(\eta, \vec{\Omega}_f)$$

$$\vec{\nabla} \cdot \vec{u} = 0$$

Torque Balance approach (Busse 1968, Noir et al 2003, Noir and Cebron 2015)

$$I_c \frac{d\vec{\Omega}_t}{dt} = \vec{\Gamma}_i + \vec{\Gamma}_p + \vec{\Gamma}_\nu + \vec{\Gamma}_{prec}$$

$$F(\vec{\Omega}_f) = \vec{0}$$

$$\vec{\Gamma}_\nu = K(\vec{\Omega}_s - \vec{\Omega}_f)$$

$$K = I_c \lambda_l \sqrt{E}$$

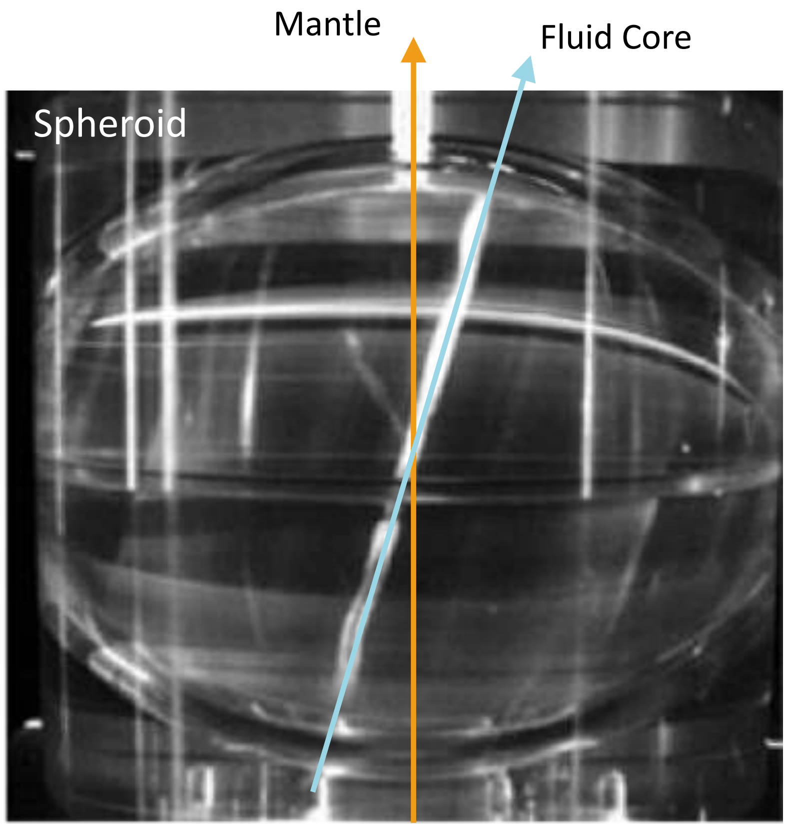

Uniform Vorticity Flow:

The primary response of the fluid to the precession of the core and mantle consist in a tilted rotation. Following Noir et al. 2003 or Busse 1968, one can derive the equation governing the three components of the fluid rotation vector:

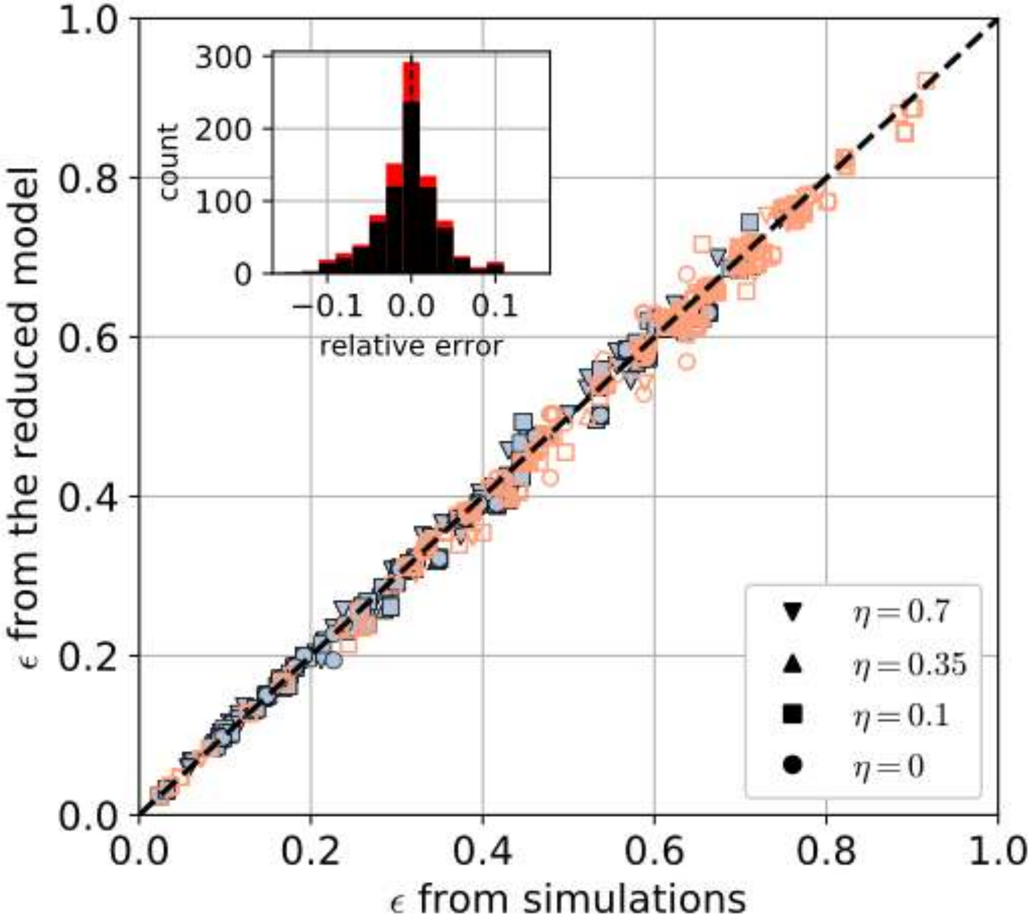

$$\mathbf{U} = \mathbf{\Omega_f} \times \mathbf{r}$$

$$\begin{aligned}
\Omega_z &= \Omega_x^2 + \Omega_y^2 + \Omega_z^2, \\
-P_z\, \Omega_y &= (\lambda_r\, \Omega_x \Omega_z^{1/4} + \lambda_i\, \Omega_y \Omega_z^{-1/4})\sqrt{E}, \\
P_x\, \Omega_y &= -\lambda_r\, \Omega_z^{1/4}\,(1 - \Omega_z)\,\sqrt{E},
\end{aligned}$$

$$\underline{\lambda} \approx \left[\underline{\lambda}_{inv}^{sphere} - 1.36E^{0.27} + \mathrm{i}\,1.25E^{0.21}\right] \frac{1+\eta^4}{1-\eta^5},$$

$$\mathbf{\Omega_f} = [\Omega_f^x, \Omega_f^y, \Omega_f^z]$$

$$\epsilon = |\mathbf{\Omega_f} - \mathbf{\Omega_s}|$$

The fluid core is **decoupled** from the mantle due to the rapid precession, it rotates essentially **along the normal to the ecliptic**, inclined by 1.5deg with respect to the mantle axis.

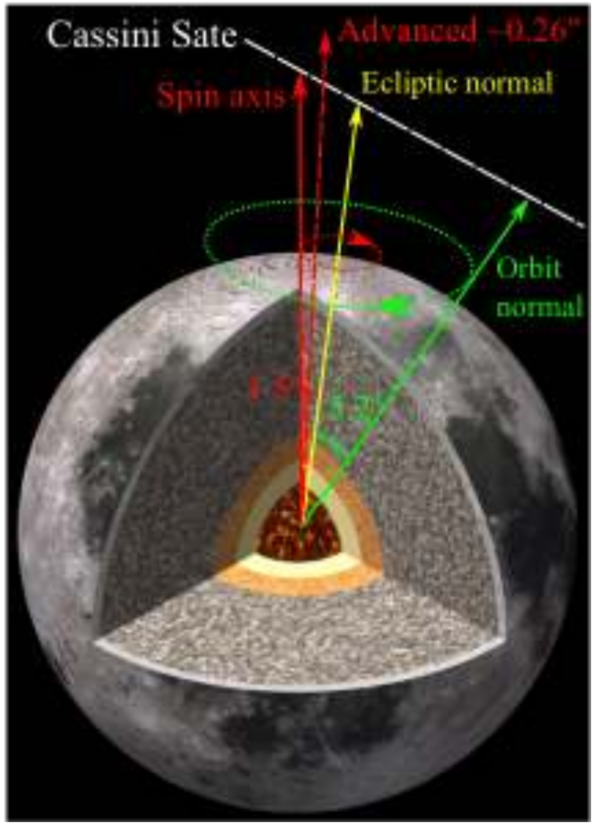

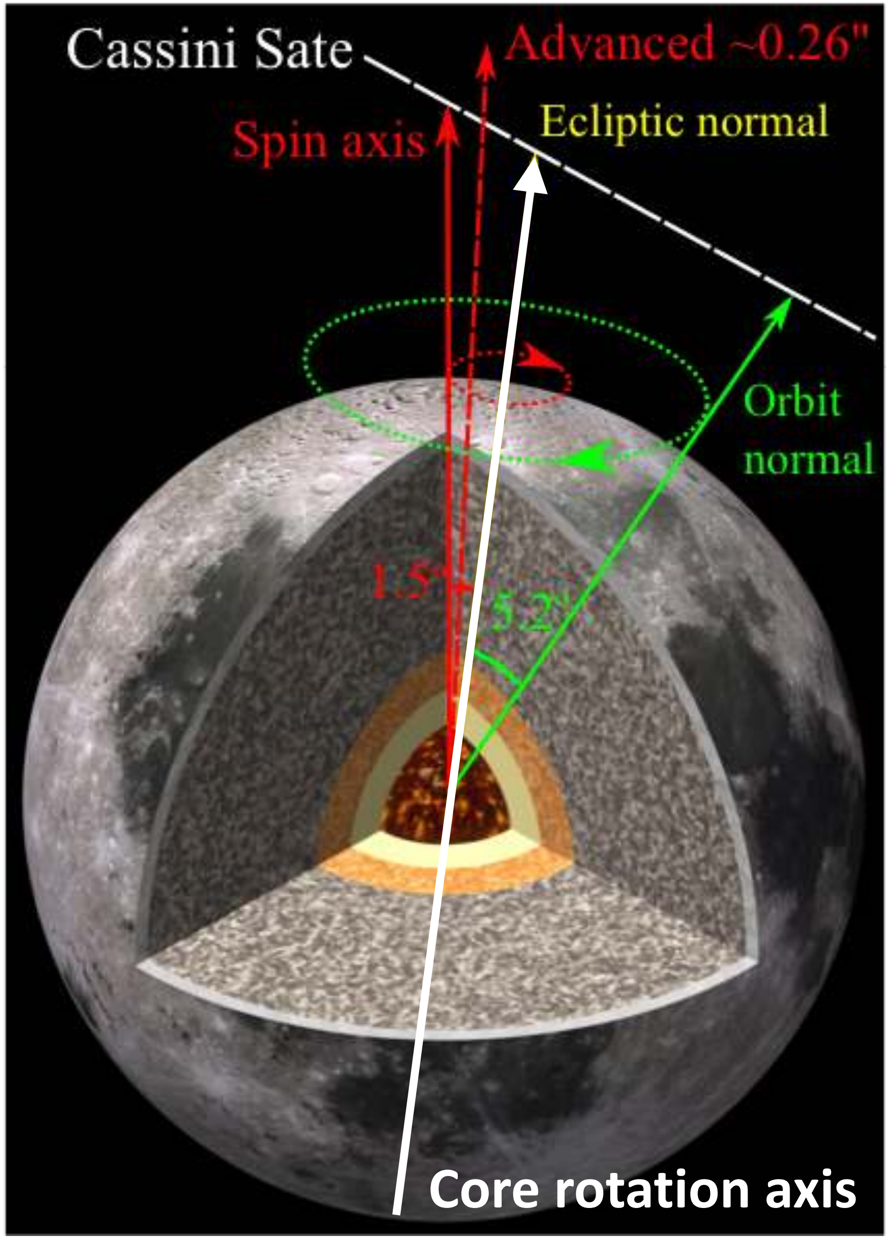

$$\frac{|\Omega_s - \Omega_f|}{\Omega_s} \sim 3 \times 10^{-2}$$

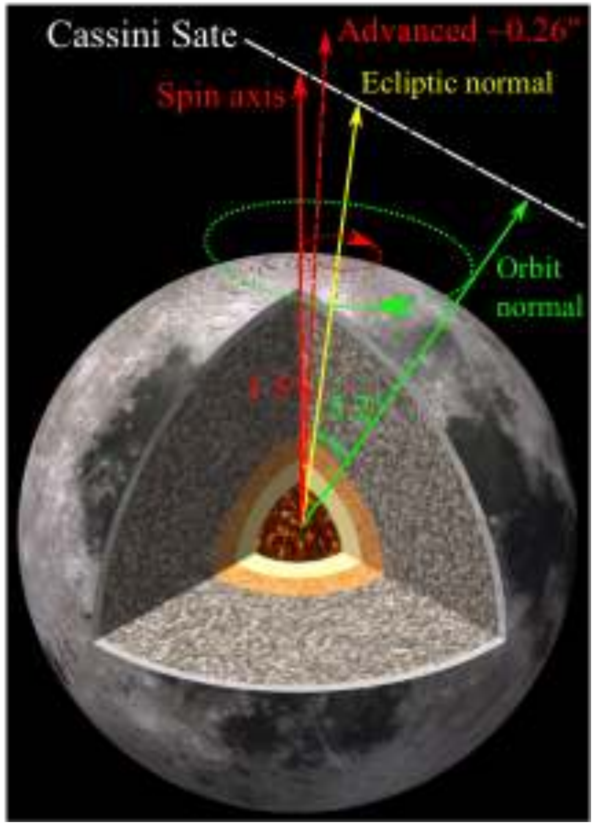

The large inclination results in a **significant differential rotation** between the lunar core and the mantle.

If the flow is laminar, the dissipation can be estimated directly from the viscous torque due to the drag in the boundary layer.

$$\frac{|\Omega_s - \Omega_f|}{\Omega_s} \sim 3 \times 10^{-2}$$

Laminar

$$\begin{aligned}\mathcal{D} &= \vec{\Gamma}_\nu \cdot (\vec{\Omega}_s - \vec{\Omega}_f) \\ &= I_c \lambda_l \sqrt{E} \Omega_f (\vec{\Omega}_s - \vec{\Omega}_f)^2\end{aligned}$$

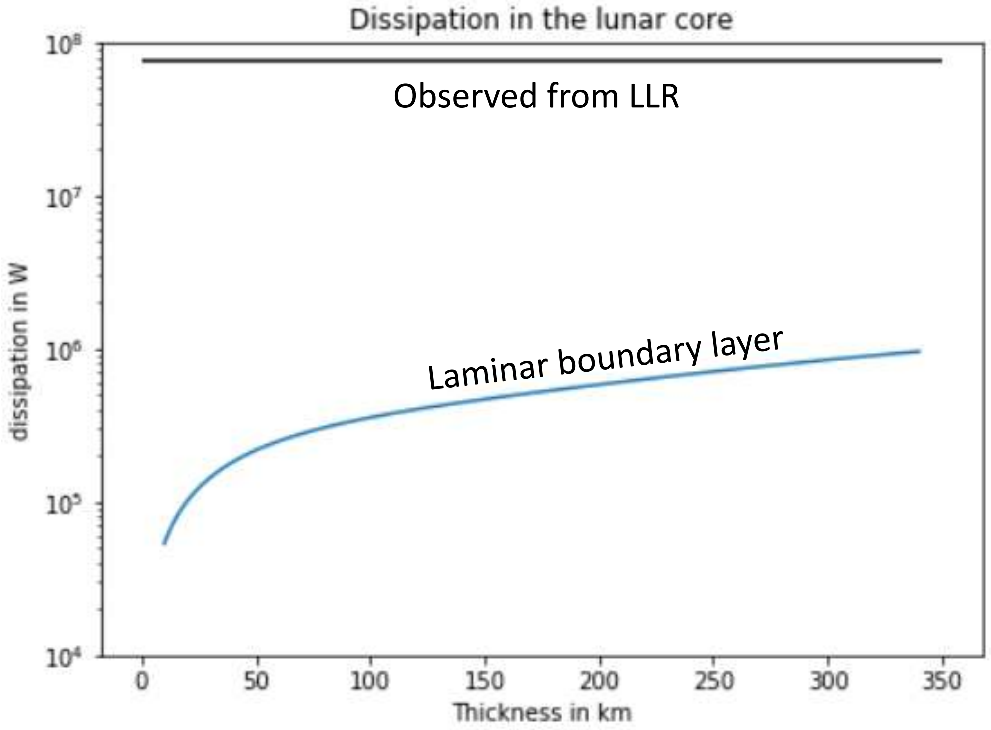

Laminar dissipation in the boundary layer cannot explain the observations.

The secondary flow driven by the Ekman pumping: What do you see if you rotate with the fluid ?

Ekman pumping driven inertial waves

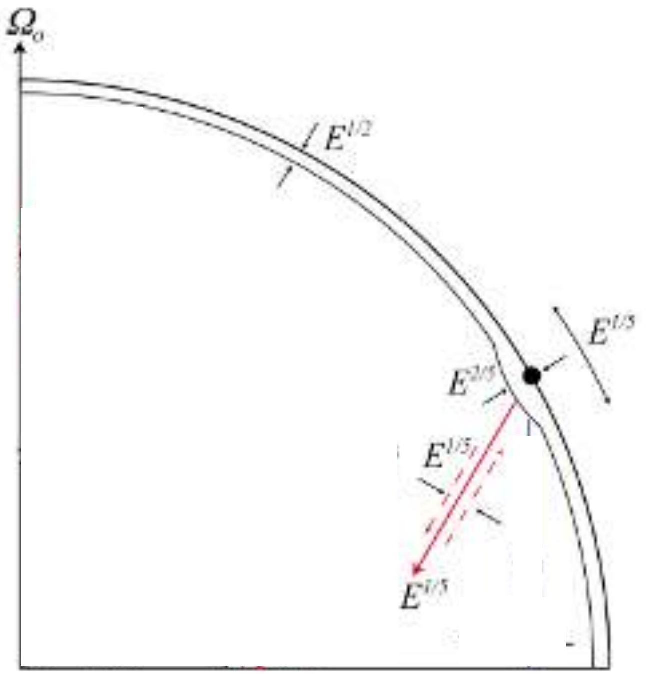

$$\sin\theta_c = \frac{\omega}{2\Omega}$$

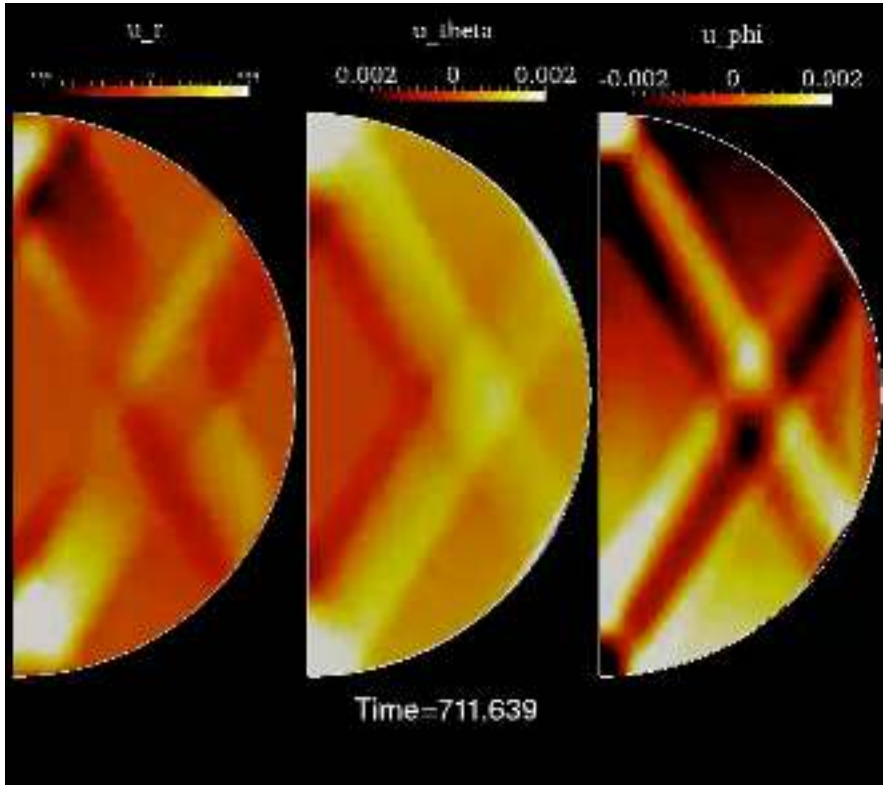

courtesy of Y. Lin

Could these oblique inertial waves dissipate enough to explain the observations ?

$$\mathcal{D}_{IW} = E \int_v |\vec{\nabla} \times \vec{u}_{shear}|^2 dV$$

The secondary flow driven by the Ekman pumping: What do you see if you rotate with the fluid ?

Ekman pumping driven inertial waves

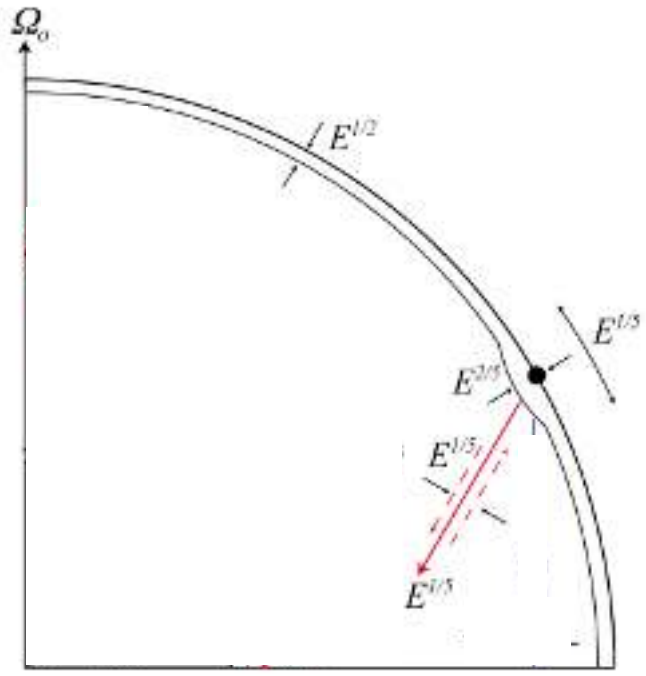

Could these oblique inertial waves dissipate enough to explain the observations ?

$$\mathcal{D}_{IW} = E\int_v |\vec{\nabla} \times \vec{u}_{shear}|^2 dV$$

$$\propto E * E^{1/5} * (E^{-1/5} E^{1/5} |\vec{\Omega}_s - \vec{\Omega}_f|)^2 \propto E^{1/10}\sqrt{E}|\vec{\Omega}_s - \vec{\Omega}_f|^2$$

$$\mathcal{D}_{IW} \propto E^{1/10}\mathcal{D}_{bl}$$

Inertial Waves:

The secondary response of the fluid to the precession of the core and mantle consist in inertial waves spawned from the critical latitudes at ICB and CMB:

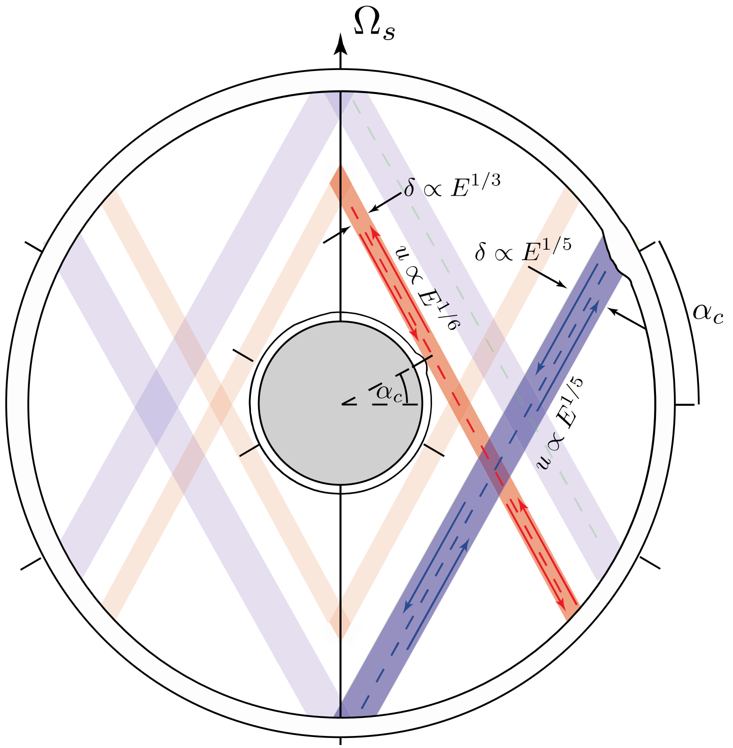

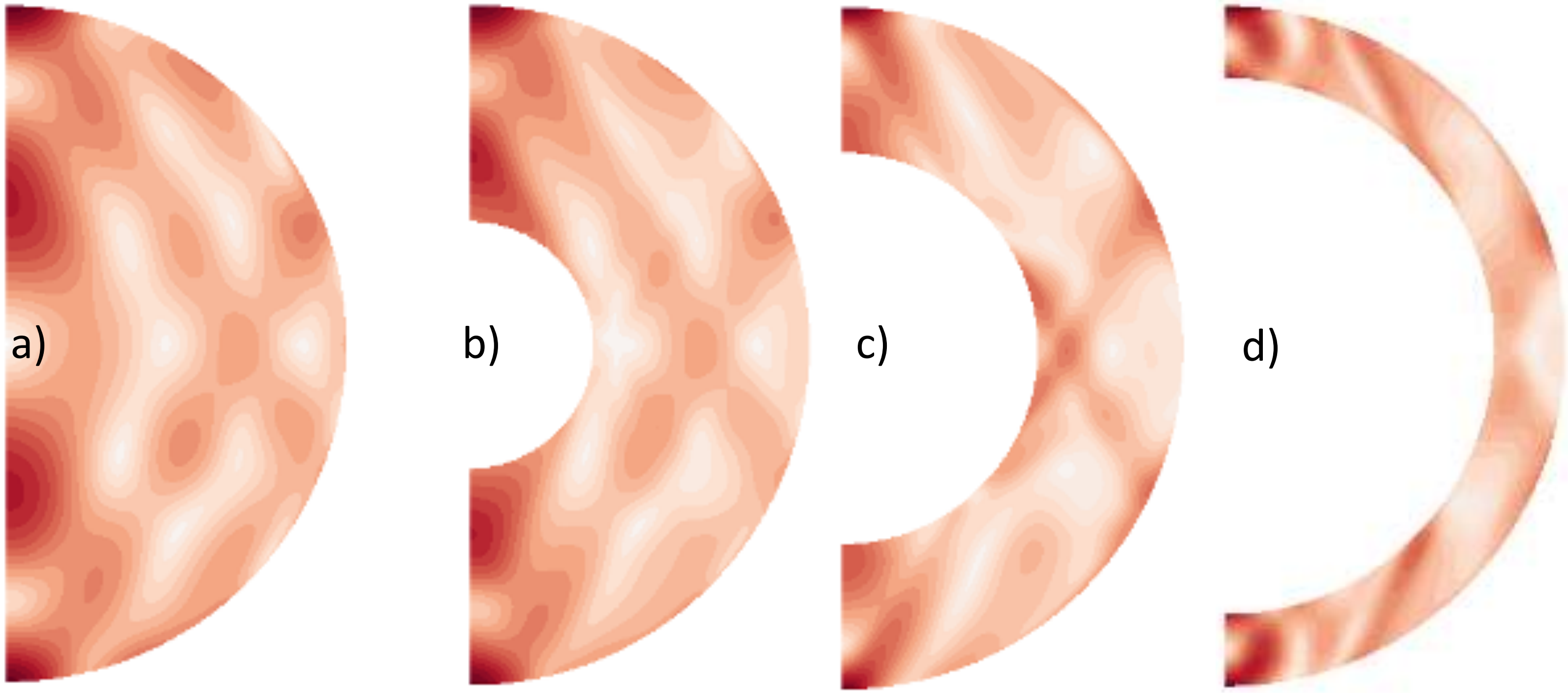

Contour plot of an instantaneous azimuthal average of the kinetic energy in the fluid frame for (a) $\eta = 0.01$, (b) $\eta = 0.3$, (c) $\eta = 0.5$ and (d) $\eta = 0.7$. In each case the flow is stable. $\alpha = 120°$, $Po = 1 \times 10^{-3}$ and $E = 3.0 \times 10^{-5}$. Contours range from 0 (white) to 0.028 (dark red)

The secondary flow driven by the Ekman pumping: What do you see if you rotate with the fluid ?

Ekman pumping driven inertial waves in the presence of an inner core

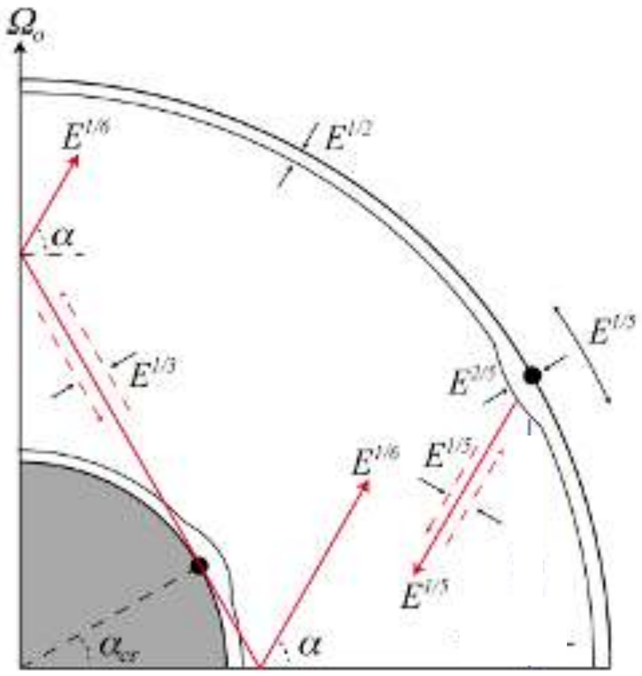

Could the oblique inertial waves spawn from the inner core explain the observations ?

$$\mathcal{D}_{IW} = E \int_v |\vec{\nabla} \times \vec{u}_{shear}|^2 dV$$

NO!

The stable flow driven by precession but also nutation, librations

$$\vec{u} = \vec{\Omega}_f \times \vec{r}$$

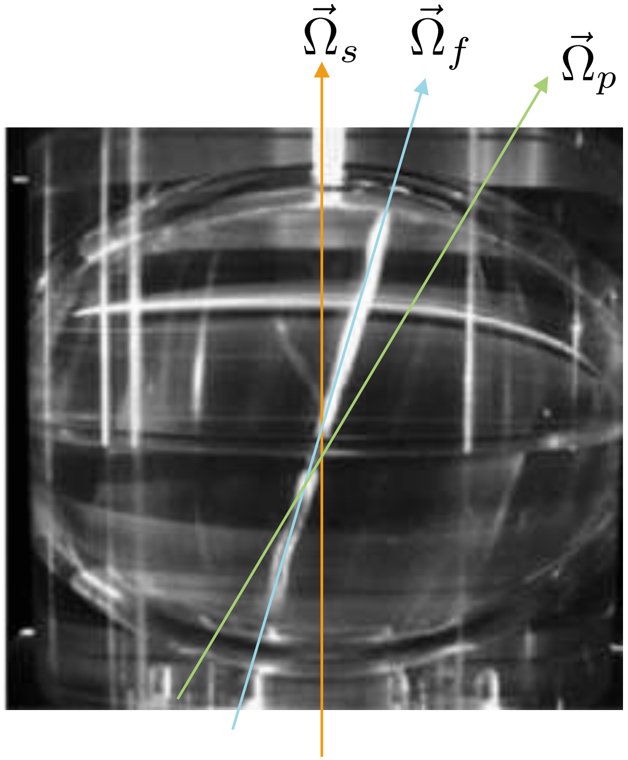

$$+\vec{\nabla}\Phi$$

elliptical deformation and planar shear of the streamlines

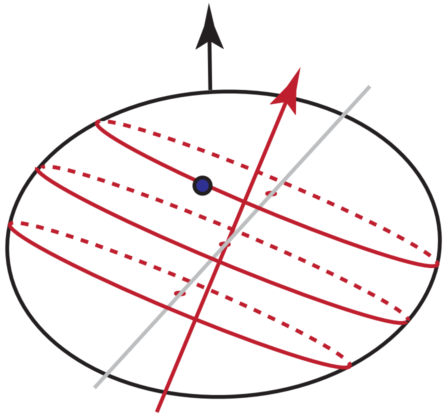

Shear of the streamlines

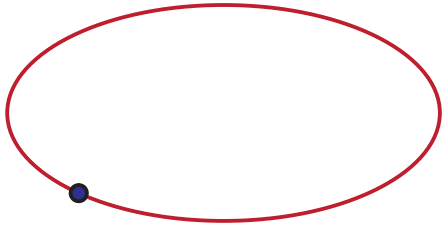

Elliptical distorsion of the streamlines

$$+\vec{U}_{IW}$$

Internal shear layer

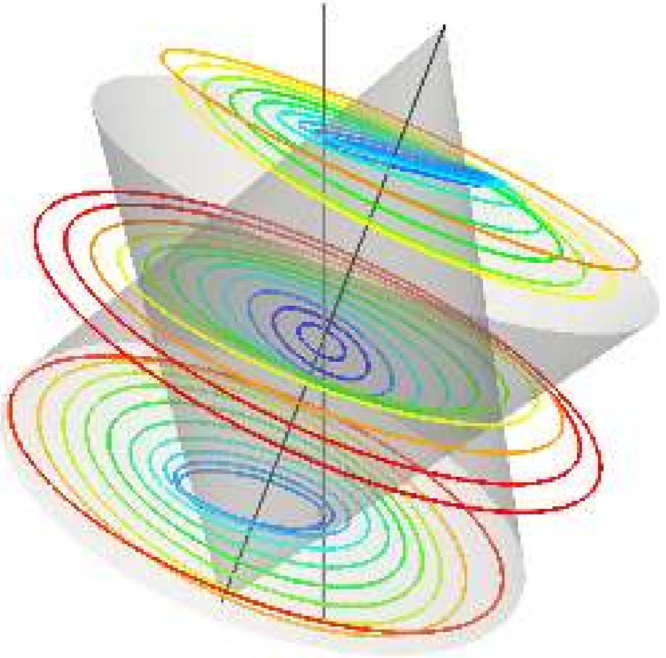

Part IV:Application to the Lunar Core.

Lecture by J. Noir at WITGAF Cargese, Corsica, 2019

1. Geophysical motivations.
2. The uniform vorticity flow.
3. Parametric versus Boundary layer instability.
4. The dynamics of lunar core over the last 4Ga.

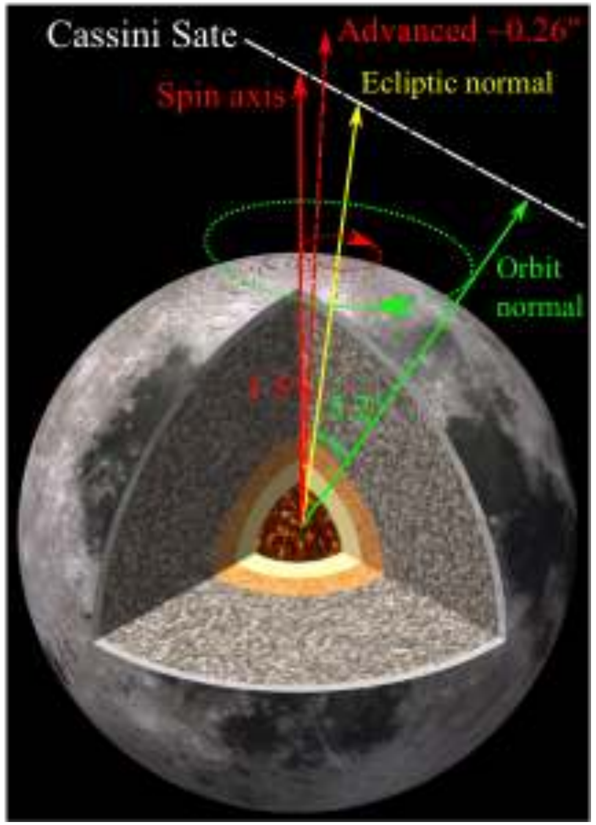

The large inclination results in a **significant differential rotation** between the lunar core and the mantle, which can drive instabilities

$$\frac{|\Omega_s - \Omega_f|}{\Omega_s} \sim 3 \times 10^{-2}$$

- **Bulk Instability**
- **Boundary layer instability**

The stable flow driven by precession but also nutation, librations

$\vec{u} = \vec{\Omega}_f \times \vec{r}$

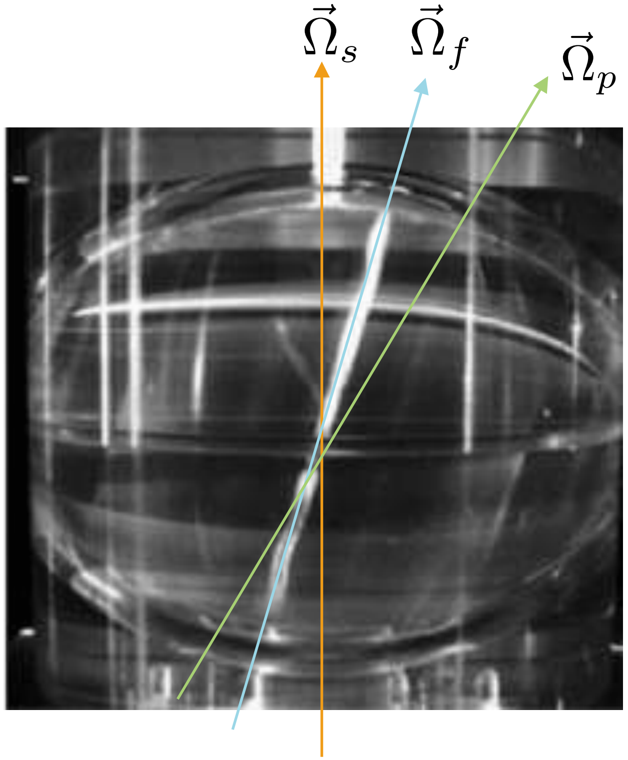

$+\vec{\nabla}\Phi$

elliptical deformation and
planar shear of the streamlines

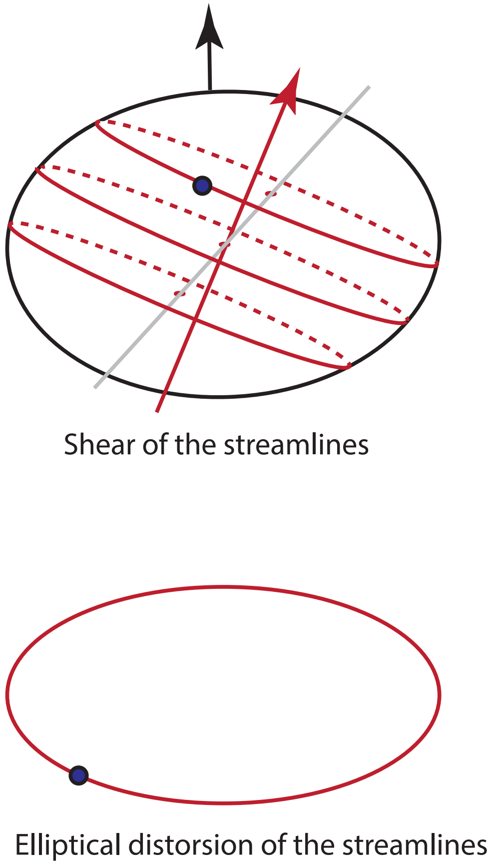

$+\vec{U}_{IW}$

Internal shear layer

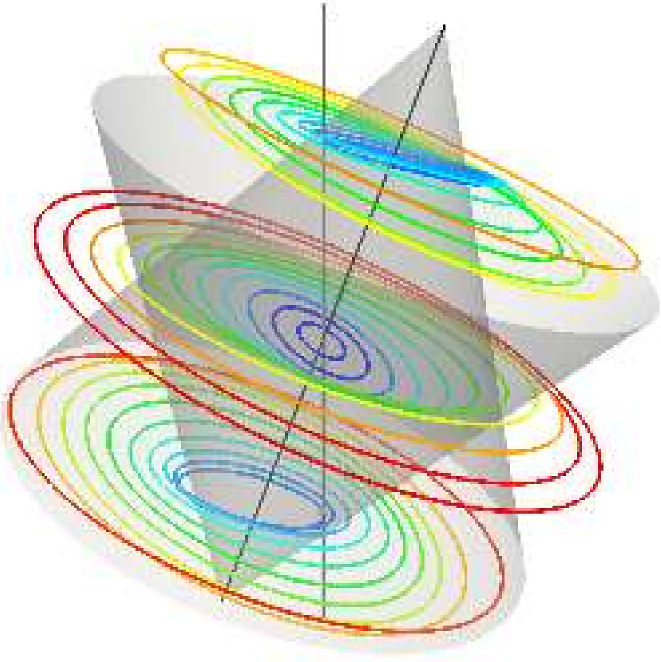

Topography driven instabilities in the bulk.
Due to elliptical deformation and planar shear of the streamlines

$$\eta \frac{\left|\vec{\Omega}_s - \vec{\Omega}_f\right|}{\left|\vec{\Omega}_s\right|} \sim \mathcal{K}\sqrt{E}$$

$\sim 3 \times 10^{-6}$ $\sim [> 1] \times 10^{-6}$

$$\eta^{1/2} \frac{\left|\vec{\Omega}_s - \vec{\Omega}_f\right|}{\left|\vec{\Omega}_s\right|} \sim \mathcal{K}\sqrt{E}^{1/4}$$

$\sim 3 \times 10^{-4}$ $\sim [> 1] \times 10^{-3}$

Kerswell 1993

Internal shear layer driven instabilities in the bulk.
exist both in ellipsoid and spherical cavities.

$$\frac{\left|\vec{\Omega}_s - \vec{\Omega}_f\right|}{\left|\vec{\Omega}_s\right|} \sim \mathcal{K}E^{3/10}$$

$\sim 3 \times 10^{-2}$ $\sim [> 1] \times 10^{-3.6}$

Goto et al. 2014, Lin et al. 2015

Topography driven instabilities in the bulk.
Due to elliptical deformation and planar shear of the streamlines

$$\eta \frac{\left|\vec{\Omega}_s - \vec{\Omega}_f\right|}{\left|\vec{\Omega}_s\right|} \sim \mathcal{K}\sqrt{E}$$

$\sim 3 \times 10^{-6}$ $\sim [> 1] \times 10^{-6}$

$$\eta^{1/2} \frac{\left|\vec{\Omega}_s - \vec{\Omega}_f\right|}{\left|\vec{\Omega}_s\right|} \sim \mathcal{K}\sqrt{E}^{1/4}$$

$\sim 3 \times 10^{-}$[illegible] $\sim [> 1] \times 10^{-3}$

Kerswell 1993

Internal shear layer driven instabilities in the bulk.
exist both in ellipsoid and spherical cavities.

$$\frac{\left|\vec{\Omega}_s - \vec{\Omega}_f\right|}{\left|\vec{\Omega}_s\right|} \sim \mathcal{K}E^{3/10}$$

$\sim 3 \times 10^{-2}$ $\sim [> 1] \times 10^{-3.6}$

Goto et al. 2014, Lin et al. 2015

Ekman Boundary layer Instabilities:

- D. R. Caldwell, C. W. V. Atta, and K. N. Helland, “A laboratory study of the turbulent Ekman layer,” Geophys. Fluid Dyn. 3, 125–160 (1972).
- Lorenzani, S., 2001. Fluid instabilities in precessing ellipsoidal shells , Ph.D. thesis, Nieders¨achsische Staats-und Universit¨atsbibliothek G¨ottingen.
- Sous, D., Sommeria, J., & Boyer, D., 2013. Friction law and turbulent properties in a laboratory ekman boundary layer, Physics of Fluids , 25 (4), 046602.

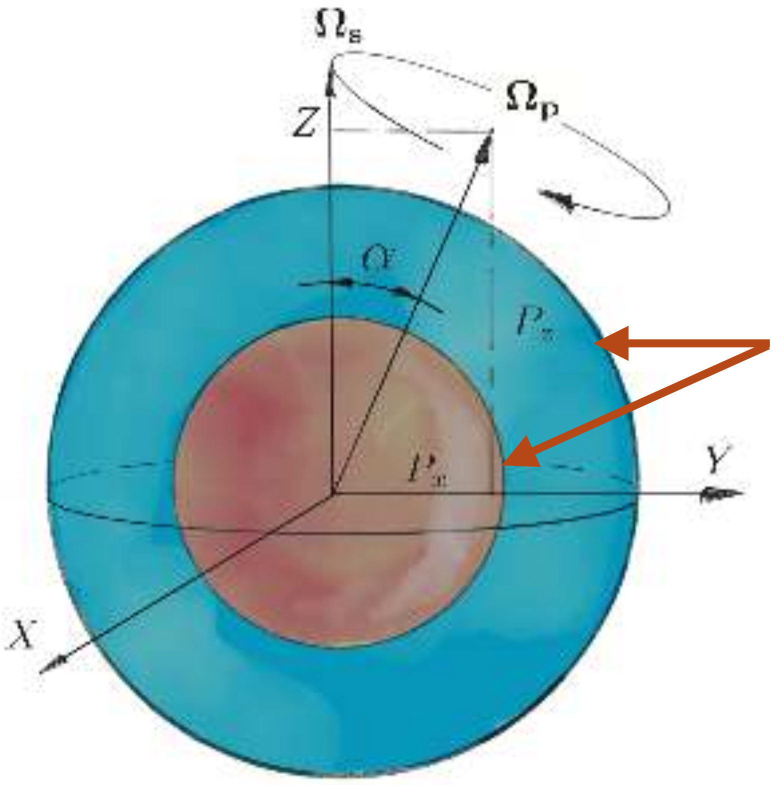

$$Re_{bl} = \frac{U_{bl}L}{\nu} \sim \frac{\left|\vec{\Omega}_s - \vec{\Omega}_f\right|}{\left|\vec{\Omega}_s\right|}\sqrt{E}$$

046602-8 Sous, Sommeria, and Boyer Phys. Fluids **25**, 046602 (2013)

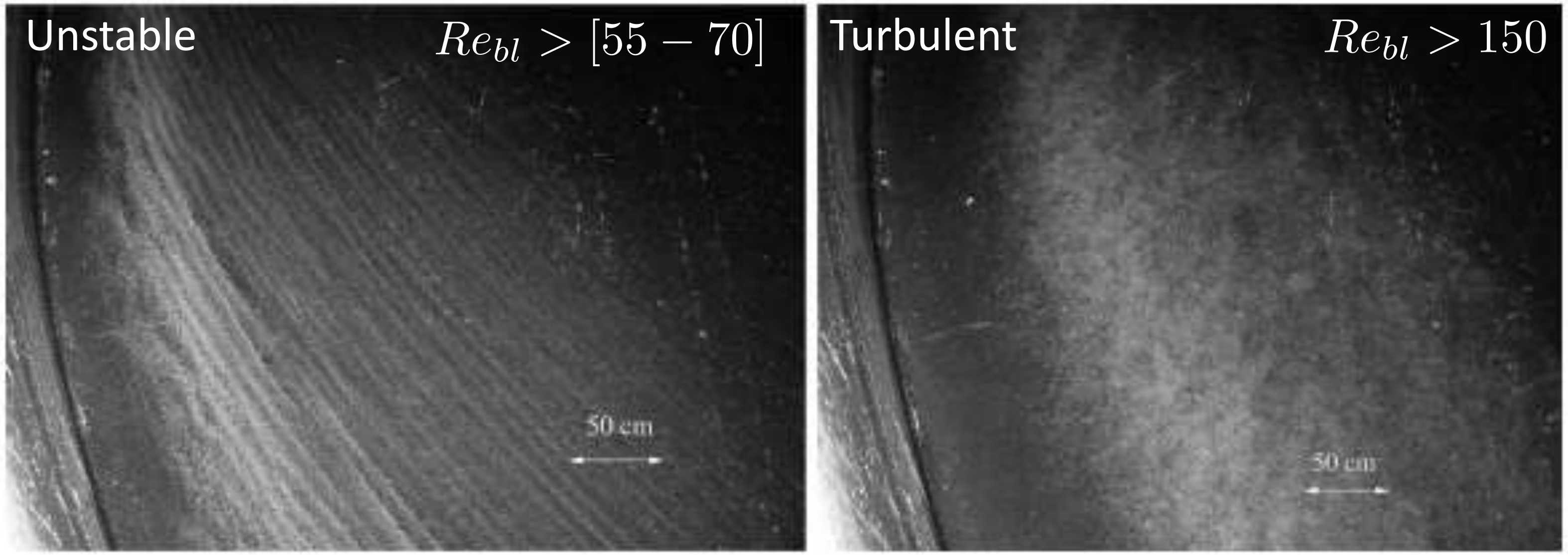

FIG. 3. Snapshots taken during the SD30-60-H66 spin-down case. (Left) Top view of instabilities in the Ekman layer developing during the initiation of the spin-down flow at $t = 2$ s after the flow initiation. (Right) Top view of the fully turbulent Ekman layer at $t = 42$ s after the flow initiation.

Numerical simulations in spherical shell: Cebron et al. 2019

parametric instability Boundary Layer instability Re>55,70

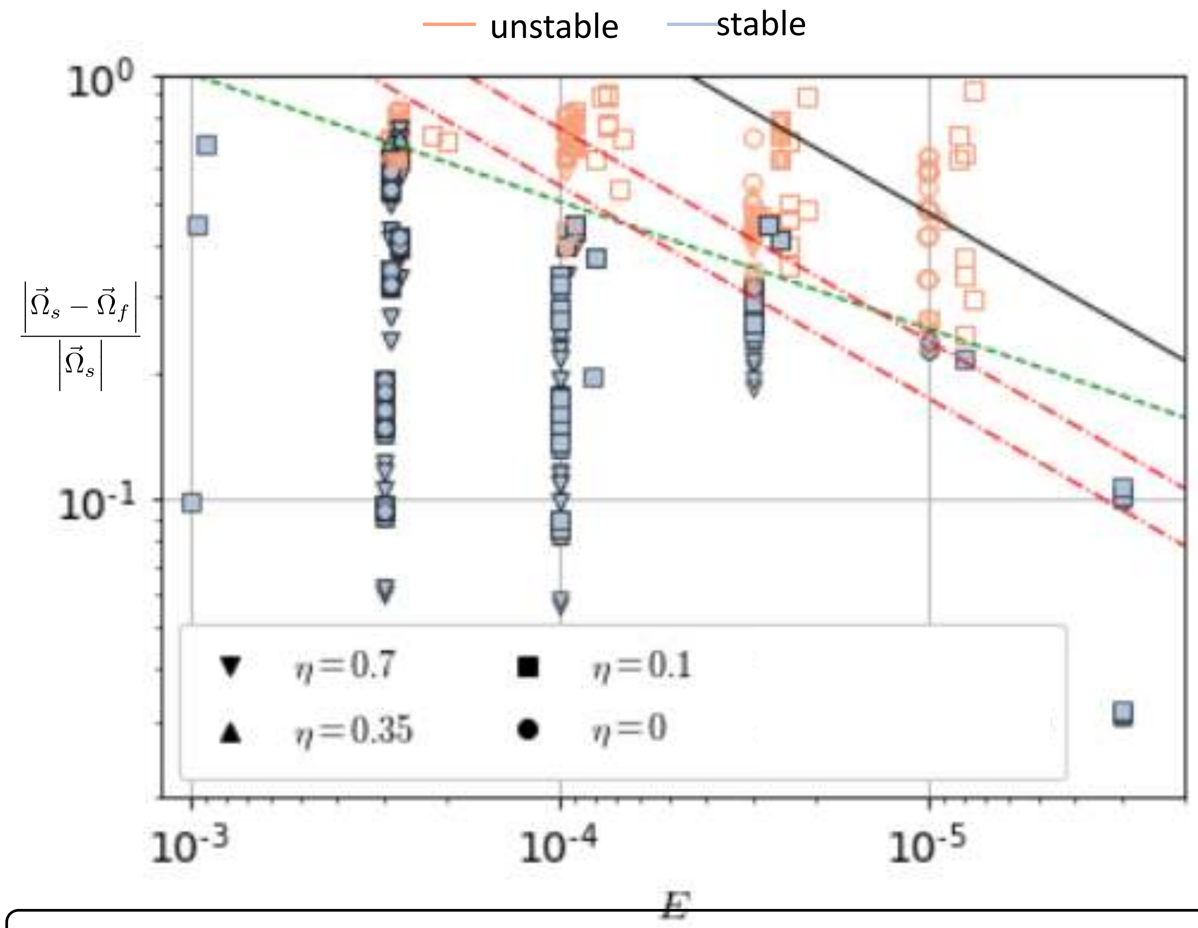

At moderate E suggest the thresholds of the parametric and boundary layer instabilities are comparable, it is difficult to distinguish between the two mechanisms.

Could boundary layers become dominant at lower Ekman numbers ?

What happens at planetary settings ?

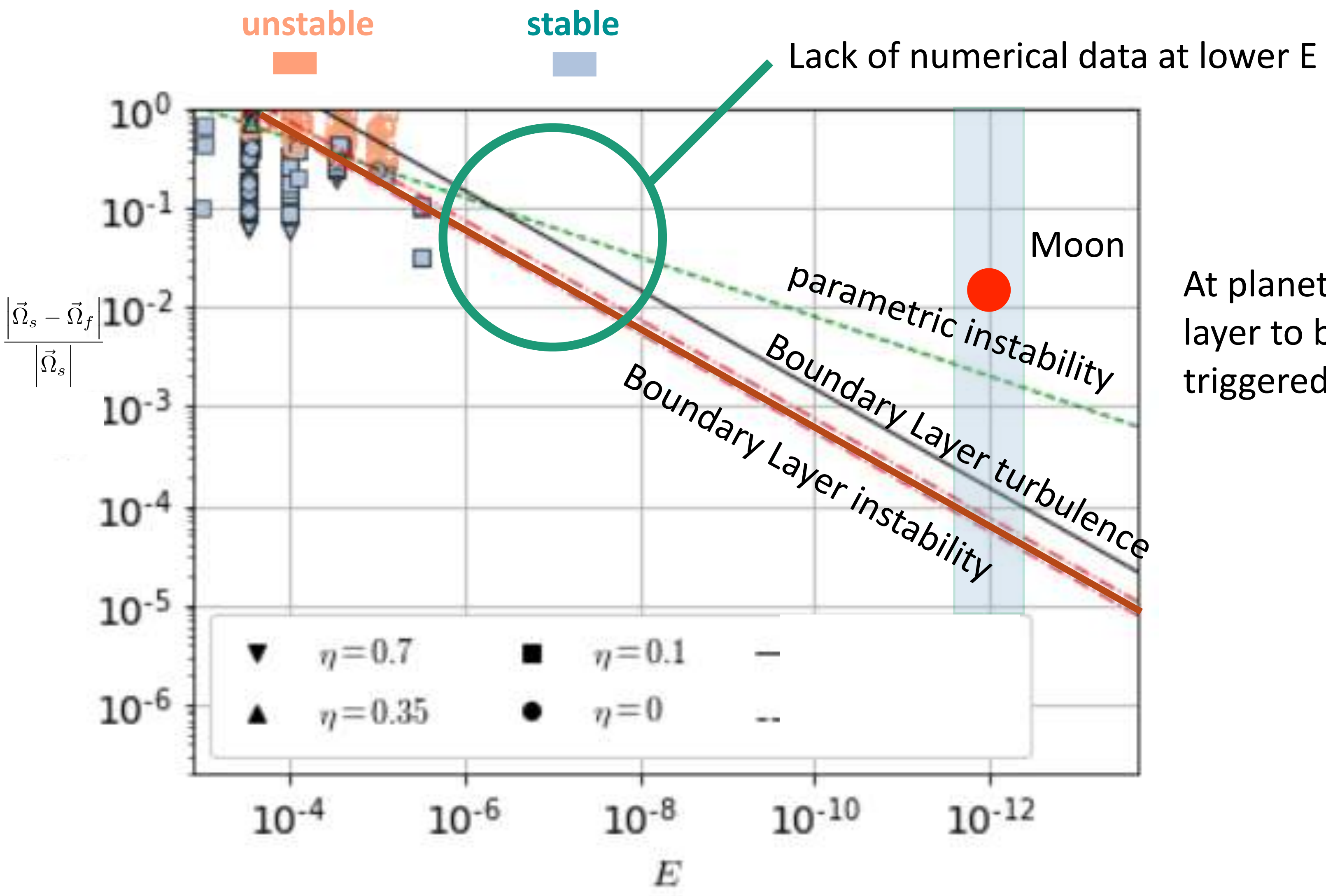

At planetary settings, we expect the Ekman boundary layer to be turbulent before a parametric instability is triggered in the bulk.

Boundary layer instability gives a lower bound estimate.

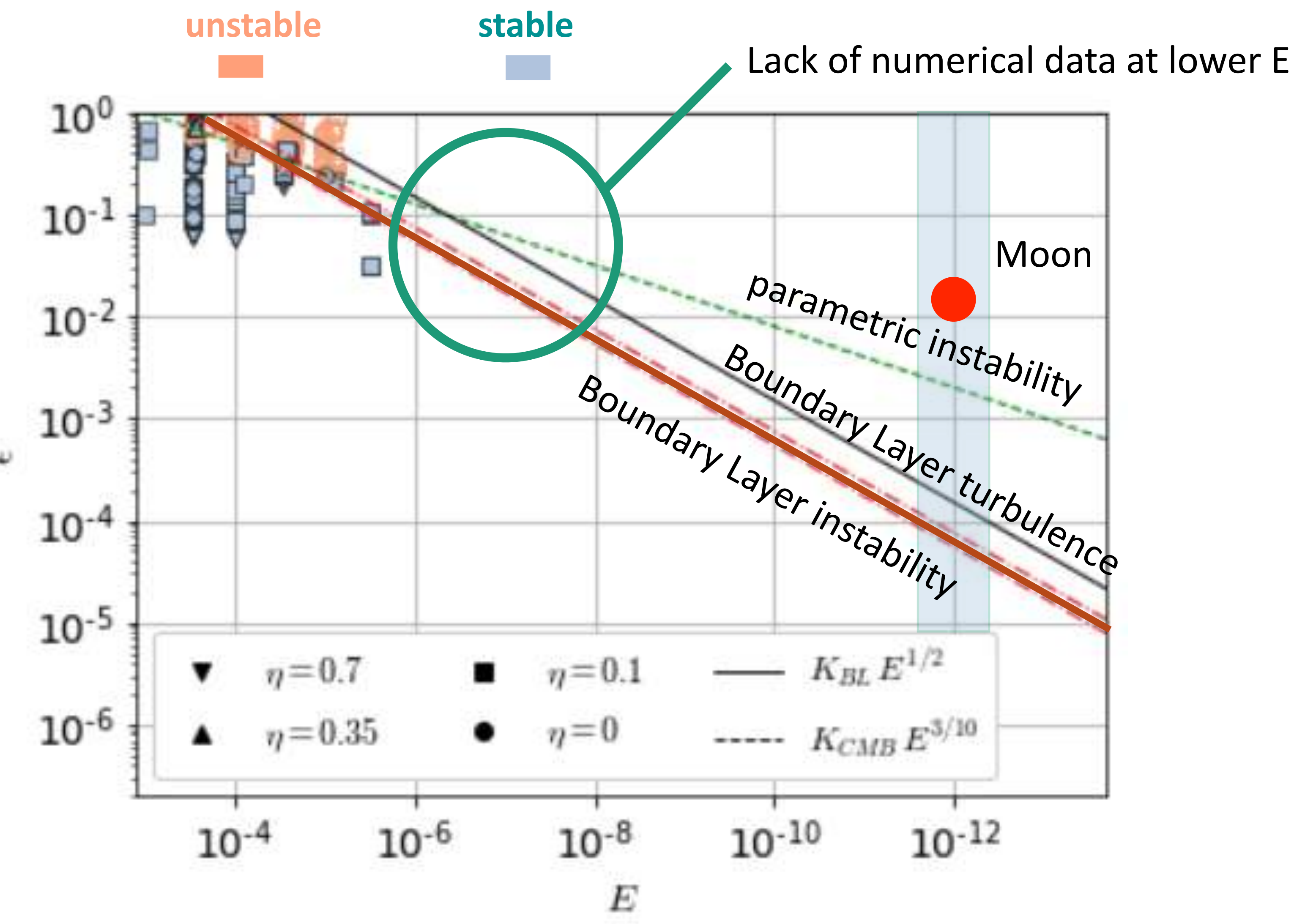

$$\vec{\Gamma}_\nu = K(\vec{\Omega}_s - \vec{\Omega}_f)$$

$$K = I_c \lambda_t \frac{\left|\vec{\Omega}_s - \vec{\Omega}_f\right|}{\left|\vec{\Omega}_s\right|}$$

$$\mathcal{D} = \vec{\Gamma}_\nu \cdot (\vec{\Omega}_s - \vec{\Omega}_f)$$

$$\mathcal{D} = I_c \lambda_t \frac{\left|\vec{\Omega}_s - \vec{\Omega}_f\right|^3}{\left|\vec{\Omega}_s\right|}$$

Cebron et al. 2019,
Sous et al. 2013

No estimate of the parametric driven dissipation.

Lack of numerical data at lower E

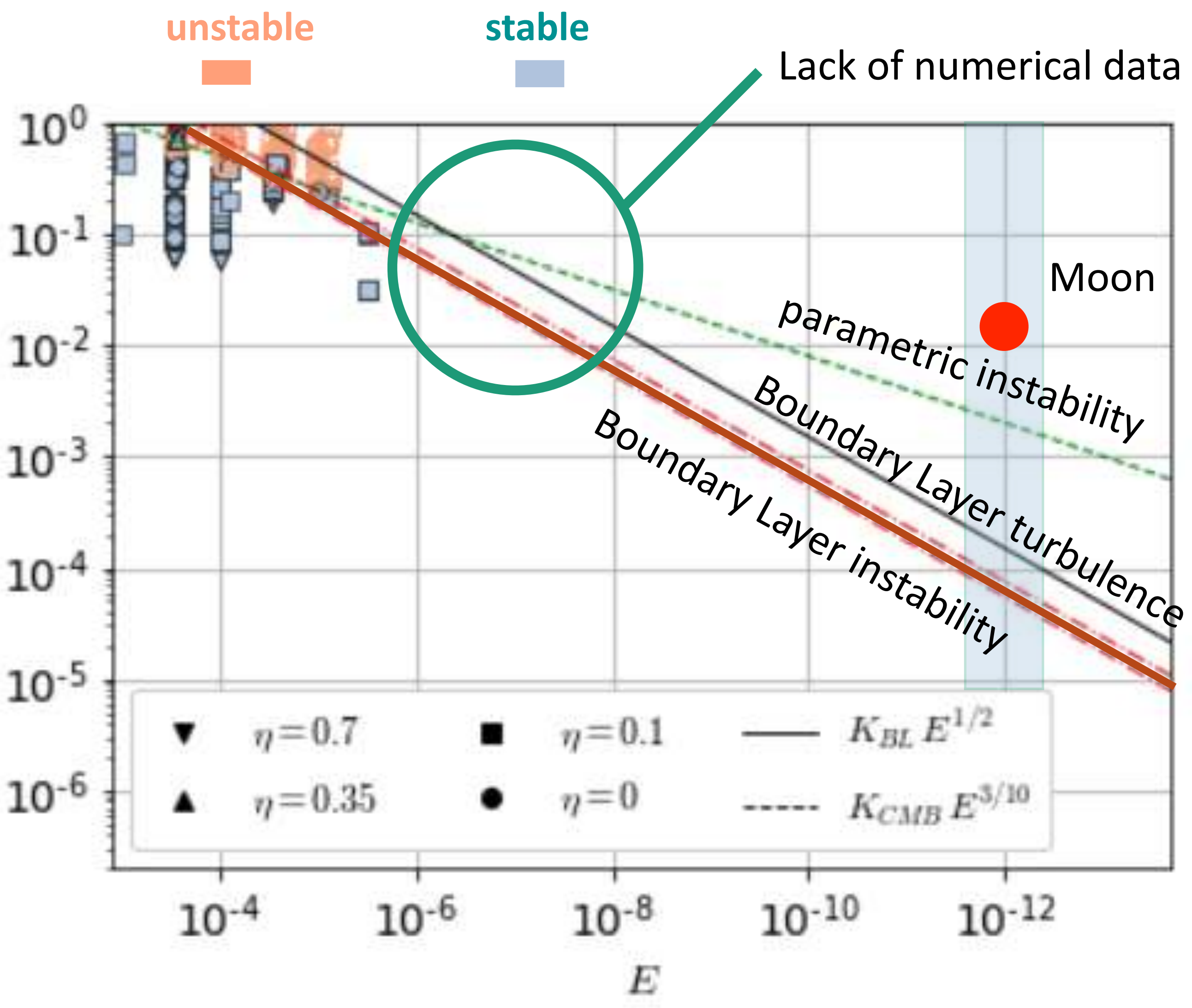

$K \propto ?$

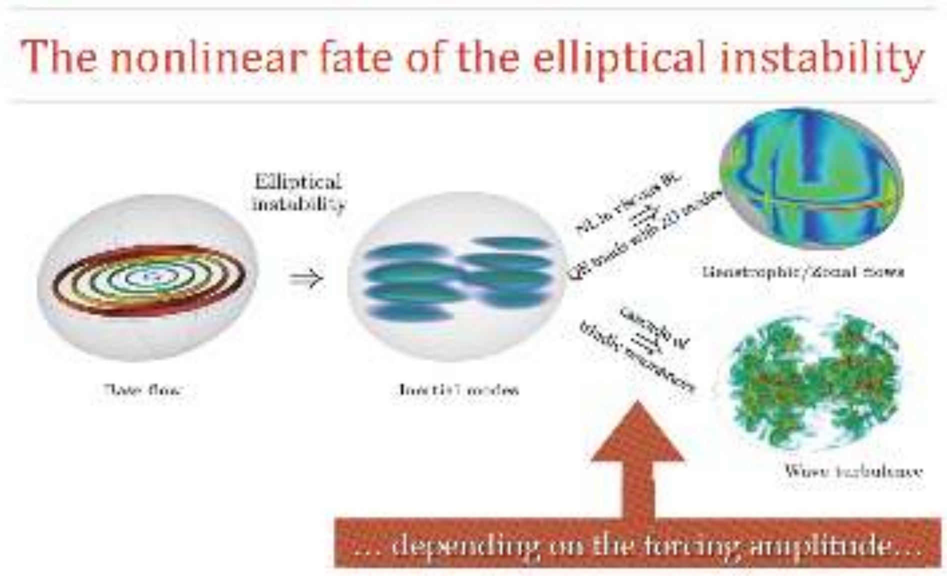

As of now, we do not have any model of the dissipation associated with a parametric resonance, neither at onset or beyond.

Numerical simulations in spherical shell: Cebron et al. 2019

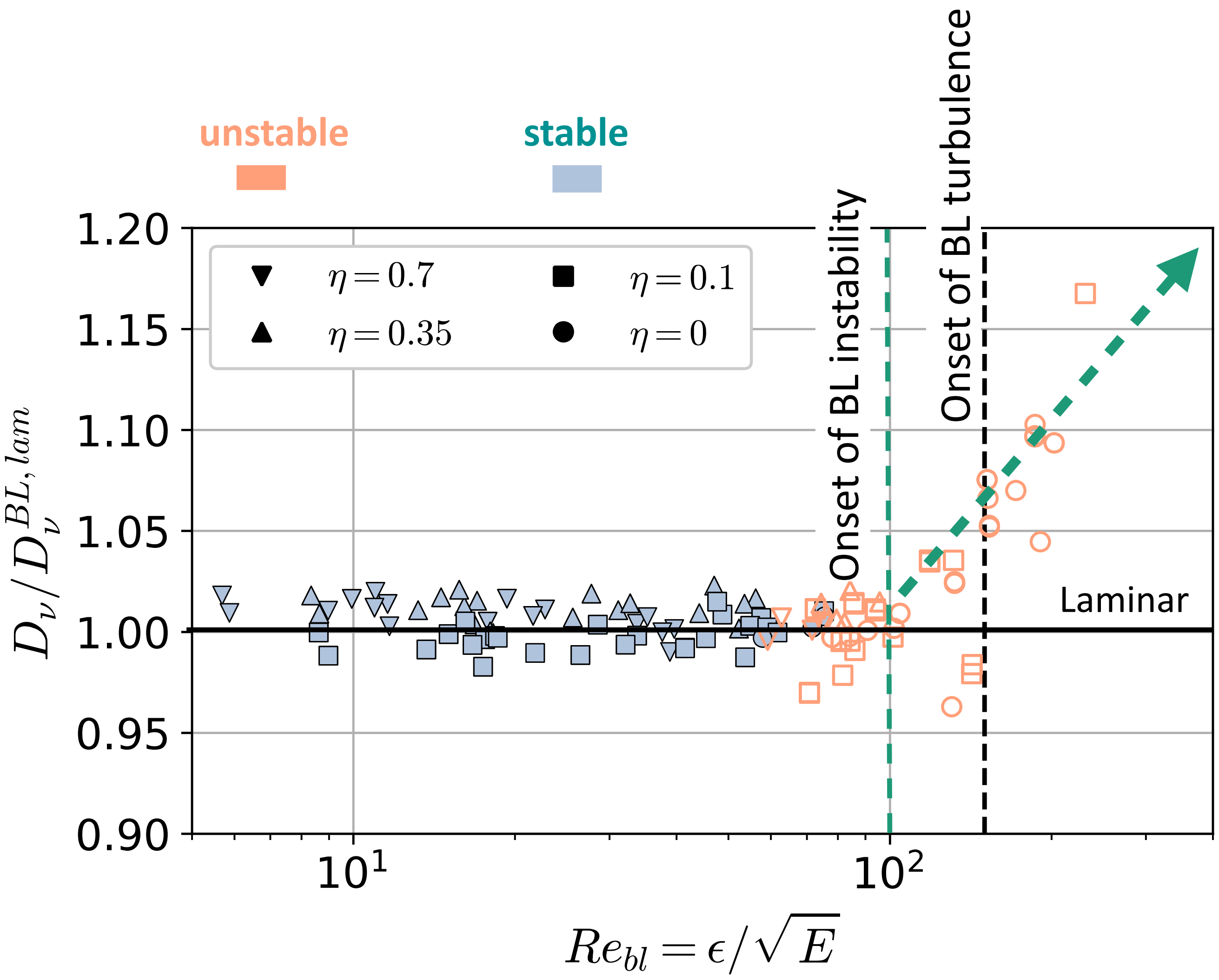

For Re_{bl}>150, Sous et al. (2013) predict turbulence in the boundary layer to enhance the dissipation:

$$D_\nu = -I_c \lambda_t \epsilon^3,$$

Instead of $D_\nu^{BL,lam} = -I_c \epsilon^2 \lambda_r \sqrt{E}.$

Even when CSI instability is present, the dissipation is still well captures by a purely laminar model. It departs from this for Re_{bl} > 125, which would be compatible with Sous et al. 2013. To conclude if this corresponds to an enhanced boundary layer or bulk dissipation one would need to perform calculation at much lower Ekman numbers.

Increase of dissipation correlates with the onset of boundary turbulence.

Part IV:Application to the Lunar Core.

Lecture by J. Noir at WITGAF Cargese, Corsica, 2019

1. Geophysical motivations.
2. The uniform vorticity flow.
3. Parametric versus Boundary layer instability.
4. The dynamics of lunar core over the last 4Ga.

Turbulent boundary layer dissipation in the Lunar core

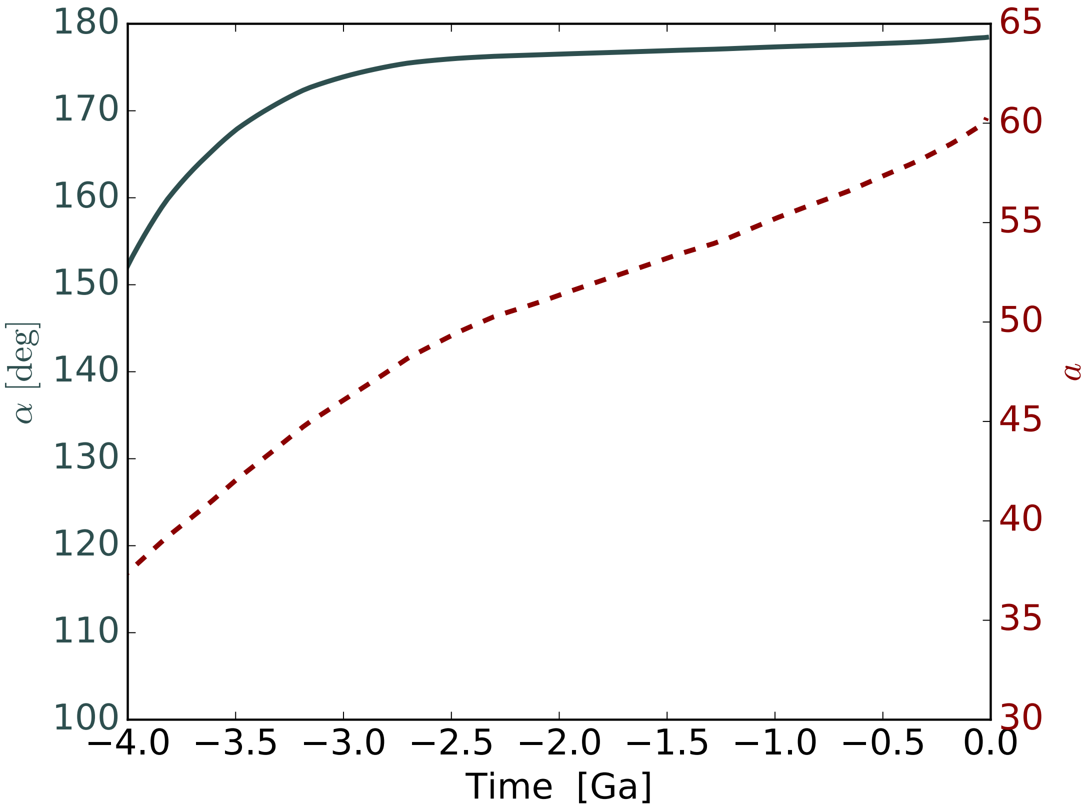

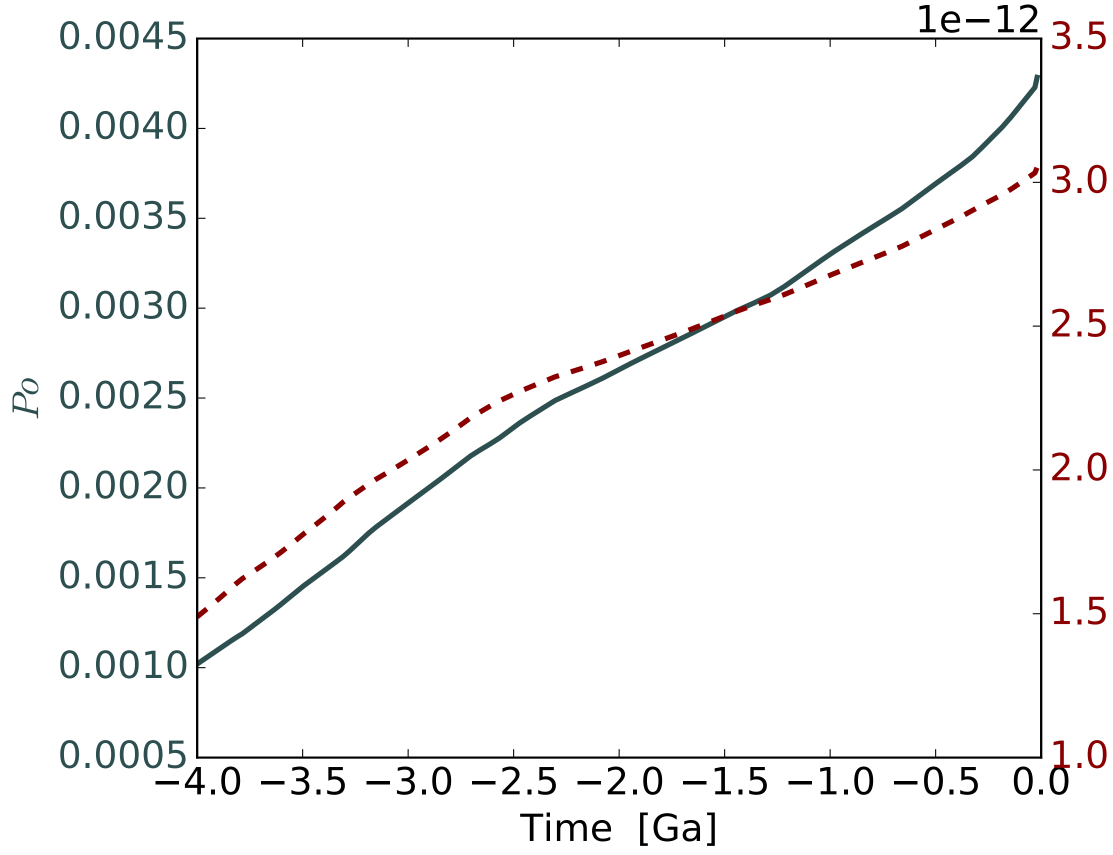

Cebron et al. 2019

Turbulent boundary layer dissipation in the Lunar core

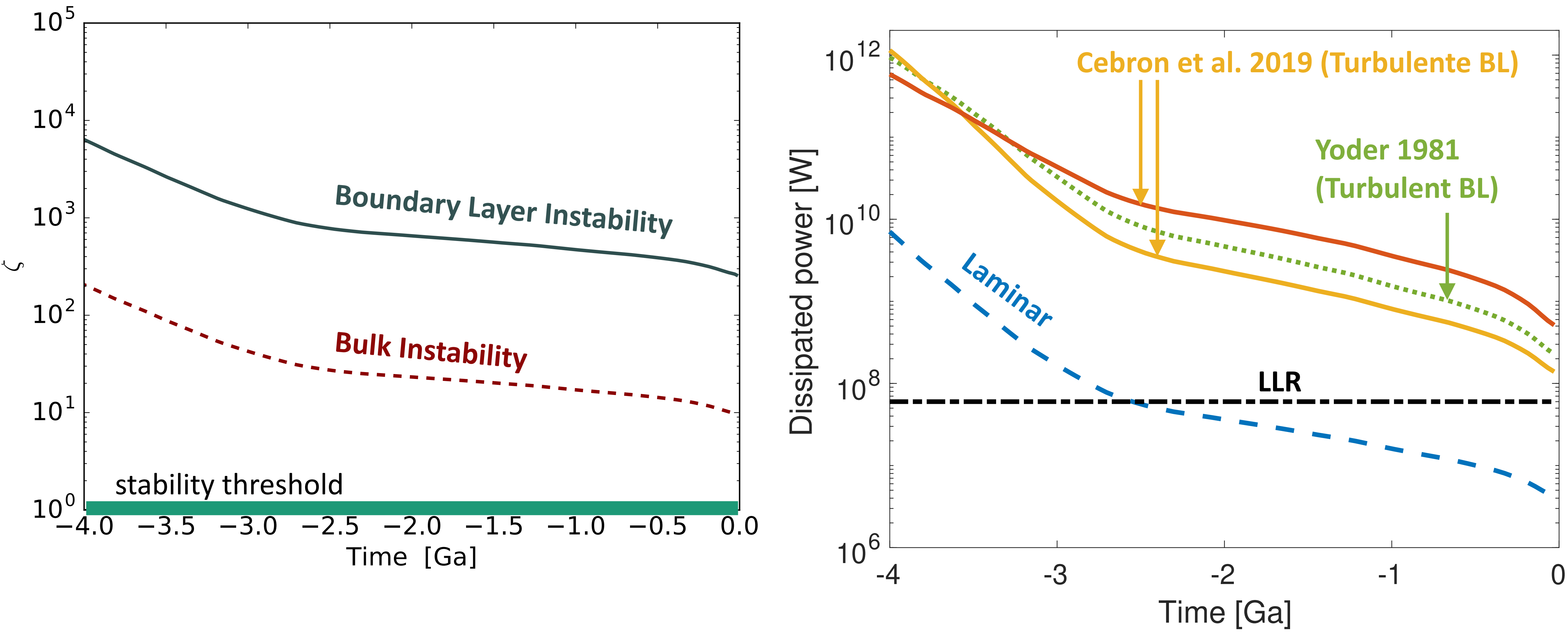

Cebron et al. 2019

Turbulent boundary layer dissipation in the Lunar core

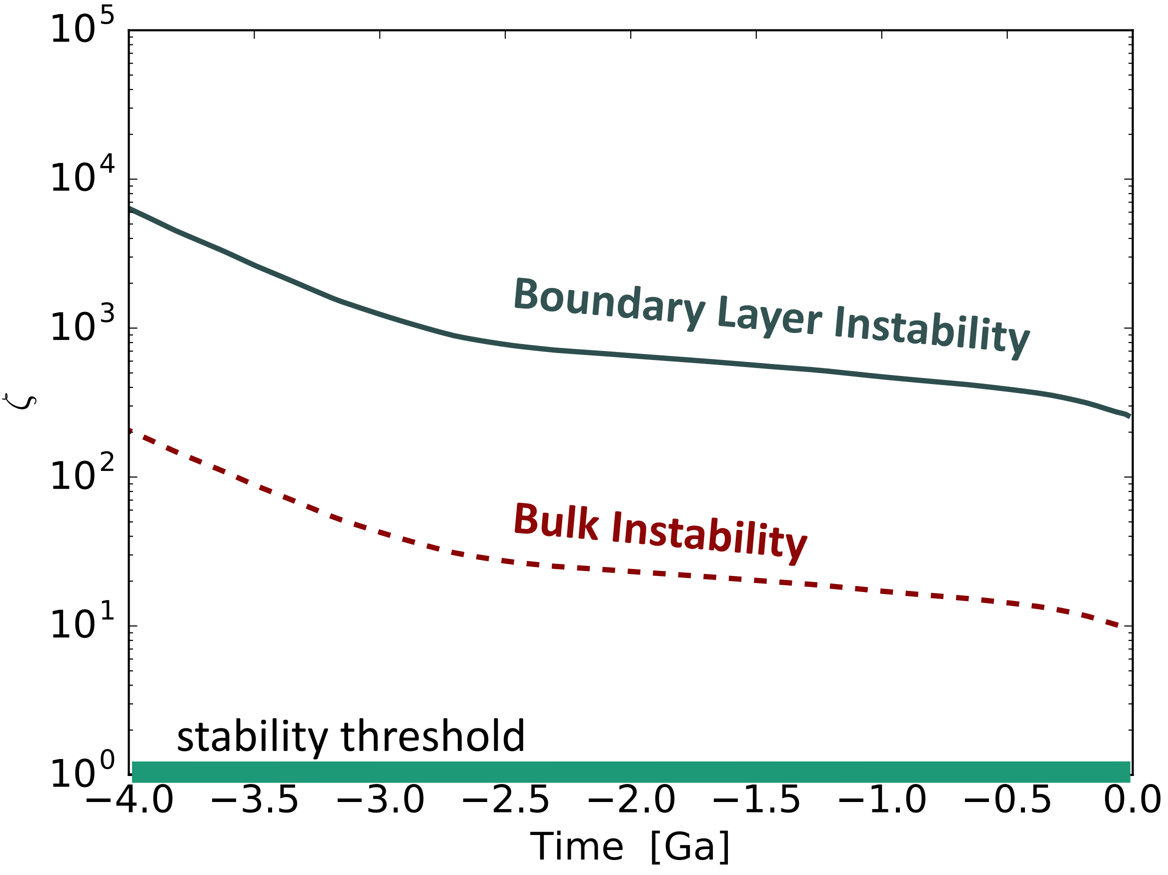

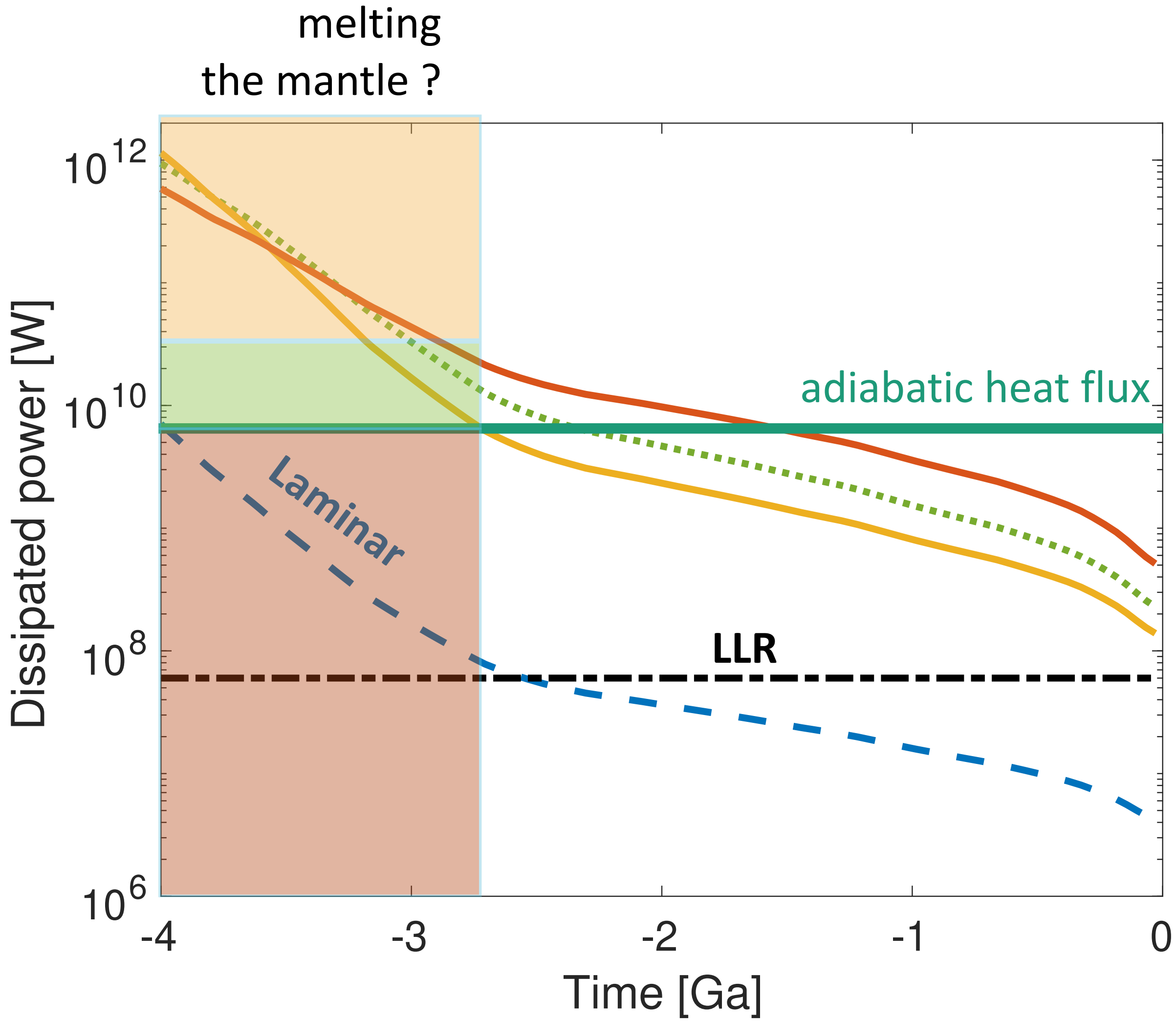

Cebron et al. 2019

Sensitivity to the core size

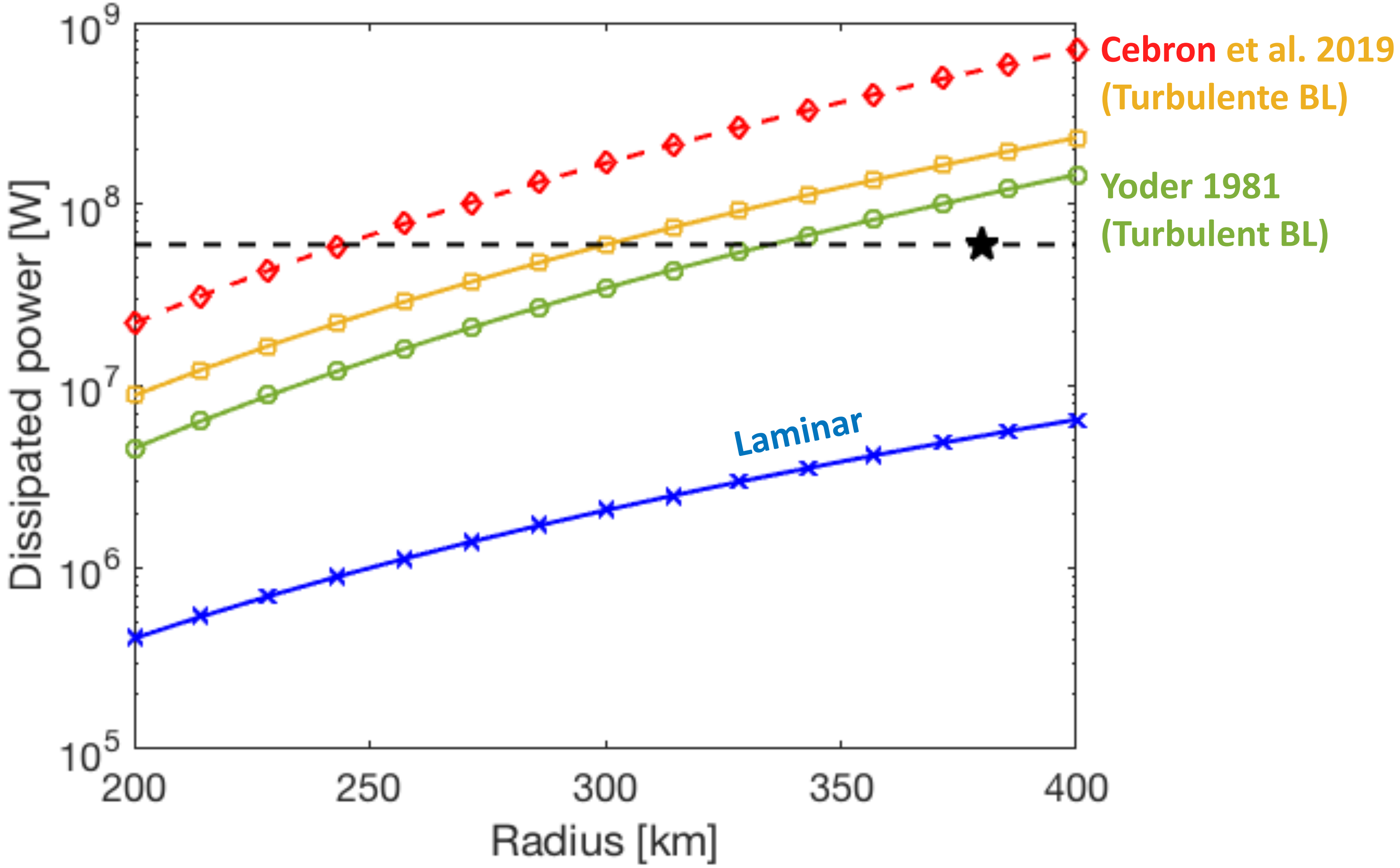

Cebron (personal communication)

Take away message

-Lower bound of precession driven dissipation:

- **Laminar core or sub-surface ocean:**

$$K = I_c \lambda_{lam} \sqrt{E} \qquad \mathcal{D} = I_c \lambda_{lam} \frac{\left|\vec{\Omega}_s - \vec{\Omega}_f\right|^2}{\left|\vec{\Omega}_s\right|} \sqrt{E}$$

- **Turbulent boundary layer:**

$$K = I_c \lambda_t \frac{\left|\vec{\Omega}_s - \vec{\Omega}_f\right|}{\left|\vec{\Omega}_s\right|} \qquad \mathcal{D} = I_c \lambda_t \frac{\left|\vec{\Omega}_s - \vec{\Omega}_f\right|^3}{\left|\vec{\Omega}_s\right|}$$

-The Lunar core has been unstable over its entire history, with tidal power as large as 10’sGW to TW in its early stage, enough to power a dynamo…